Fiber Finishes for Improving Interfacial Thermo-Oxidative Stability in PMR-II-50 Matrix Composites

Final Report
For the Period of October 1993 through September 1996
Contract NAS3-27090

Prepared for
NASA-Lewis Research Center
Cleveland, OH 44135

Prepared by
Dr. Ronald E. Allred
Dr. Larry A. Harrah
Adherent Technologies, Inc.
9621 Camino del Sol NE
Albuquerque, NM 87111

and

Dr. Thomas A. Donnellan
Mr. Theotis Williams, Jr.
Dr. Raymond Meilunas
Northrop Grumman Corporation
Advanced Technology Development Center
Bethpage, NY 17114

CONTENTS

FIGURES

FIGURES
(concluded)

TABLES

Executive Summary

The integrity of the interface is a controlling factor in the performance of high-temperature polymer matrix composites. Commercially available sizings or finishes have been shown to be inadequate for achieving the 30,000-hour lifetime goals for composite engine components. To improve the interface, an ideal finish for these systems will uniformly coat the carbon fibers, have good thermo-oxidative stability (TOS), and chemically bond to the reinforcing fibers. The objective of this program was to demonstrate the use of a reactive coupling agent chemistry for formulating a fiber finish for PMR-II-50 polyimide matrix composites that would enhance composite interfacial TOS.

To achieve this objective, the following properties of the reactive finishes and finished composites were determined:

- reactivity with carbon fiber surfaces
- formulations for optimum bonding to polyimides
- interface properties of finished composites
- thermal stability of bulk finish castings and finished composites
- TOS of finished composites at 400, 371, and 316°C.

The overall program results were mixed. Finishes were successfully formulated that uniformly coated the individual carbon fibers and reacted with them and the polyimide matrix. The finish formulations displayed thermal stabilities near those of the neat PMR-II-50 material, and composites fabricated from them displayed mechanical properties similar to those fabricated using unsized fibers. When those composites were aged at 400, 371, and 316°C, however, only limited evidence was obtained showing that the reactive finishes protect the fibers from oxidation and improve composite TOS. The aging conditions used were too severe for the bulk composite. Consequently, changes in mechanical properties were dominated by bulk degradation of the matrix. However, evidence gathered on the aged composite fracture surfaces using scanning electron microscopy (SEM), micro-Fourier transform infrared (FTIR), dynamic mechanical analysis (DMA), and voltage-contrast x-ray photoelectron spectroscopy (VCXPS) techniques support the hypothesis that the finish improves composite TOS. The evidence supporting the potential benefits of the reactive finishes is compelling, but not proven at this point.

If these reactive finishes are proven to improve composite TOS, their use will result in composites for high-temperature applications with greater environmental durability and longer operating lifetimes.

Introduction

There is a tremendous potential for the use of polymer matrix composites in aerospace engine applications. To meet that potential, the design and development of unique, robust high-temperature composite systems has been driven by the National Aeronautics and Space Administration (NASA) and the Department of Defense (DoD). The aggressive engine environment has required new blends of materials properties in the composite fiber and matrix. Fiber manufacturers must balance thermo-oxidative stability (TOS) and fiber mechanical properties. Similarly, resin system developers must balance the TOS of the material and the processability. The most successful resin chemistry approach for high-temperature applications has been the polymerization of monomeric reactants or PMR polyimide chemistry developed at the NASA Lewis Research Center (LeRC) [1]. The PMR-15 system is the only high-temperature composite that has been used in engine structural applications that require up to 288°C operating performance. Subsequent research resulted in improved high-temperature systems such as the PMR-II-50 polyimide [2]. Widespread use of these high-temperature polymer matrix composites requires improving the long-term TOS of the composite systems in the environments that exist in conventional and next-generation engines.

The TOS of high-temperature composites is controlled by a combination of factors that include the thermal stability of the constituents, the component geometry, and the interfacial adhesion between the fiber and the resin in the material. Observations of exposed sample surfaces show that the degradation mechanisms can include global attack on both the resin and the fiber, interfacial deterioration, and microcracking in the resin [3]. Variations in the types of sample geometries and the exposure conditions used affects both the mechanism and the rate of degradation of these composites, and clouds any attempt to quantitatively compare the performance of materials examined in past studies.

In general, the TOS of newly developed materials is described by the weight loss measured as a result of exposure to some set of environmental conditions. The use of weight loss as a screening criteria for material stability relies on the belief that the material performance will not be significantly affected by exposure until chemical structural changes progress to a point at which the material deteriorates. For actual applications, the performance of high-temperature composites must be ascertained by the measurement of physical and mechanical property changes that occur as a result of exposure. Although the stabilities of the polymers and the fibers used in these high-temperature materials have improved over the last 15 years, it is often found that the improvements do not translate into composite behavior.

Scola *et al.* [4] have reported such behavior in a study of graphite fiber/PMR-15 composites in which the surface oxygen concentration of the fiber varied. Even

though the fibers with high surface oxygen concentrations degraded at relatively low temperatures, the composites produced with these fibers exhibited excellent retention of properties after thermal exposure. The authors ascribed the results to a reduction in the oxygen diffusion rate at the fiber interface caused by improved adhesion between the fiber and the resin. The reverse behavior was reported by Miller *et al.* [5] who demonstrated that poor TOS performance of some T-40R fiber-based PMR-15 composites was due to the lack of adhesion between the fiber and the resin. A recent study by Bowles *et al.* [6] on PMR-15 matrix composites concluded that fiber-matrix bonding affects TOS. They also showed that unsized shear treated fibers result in composites with TOS superior to epoxy sized or untreated fibers. Despite these observations, there has not been any significant enhancement of the interfacial characteristics of high-temperature systems. Consequently, interface-dominated degradation mechanisms continue to affect the TOS of polymer matrix composite materials.

A recently concluded industry round robin test program on sizings for high-temperature composites reached the following conclusion [7]:

> Although a significant amount of data was generated, the problems relating to fiber sizing were not solved. While some candidates show promise, none proved to be outstanding. This may have been, at least in part, due to the choice of test specimen geometry. Based on the results of this effort, additional work on fiber sizing technology for use in high-temperature plastic laminates would be justified.

The interface has often been cited as a critical parameter that controls the performance of all composites. Considerable progress has been made in the optimization of the interface region characteristics in conventional epoxy and bismaleimide (BMI) composites. Work in interface science has concentrated on the alteration of the fiber surface or on studies of the effect of specific fiber coatings on composite properties. Fiber surface modifications that have been examined include physical roughening for mechanical interlocking and chemical modification of the fiber surface [8-14]. The chemical treatments have been preferred since they afford improvement without the potential for degradation of the fiber properties that is inherent in surface roughening [10]. Electro-oxidative (shear treatment) techniques have been developed and are conventionally used in the treatment of carbon fiber surfaces in production. These treatments remove weak boundary layers from the surface and produce increased surface activity with formation of both acidic and basic moieties [15,16].

Work has also been performed on characterizing and modifying the interphase material that is present between the fiber and bulk matrix resin in the composite. This interphase can form naturally either as a result of altered chemical reaction kinetics in the region adjacent to the fiber surface [17] or as a result of the

interaction between the sizing or finish applied to the fiber before processing and the resin [18,19]. In some cases, coatings that are designed to afford specific characteristics to the composite system, such as stiffness or toughness, have been purposely applied to the fiber [20-23].

It has been found that each of these approaches can improve composite properties. The extension of the interphase modification concept through the use of reactive finishes for improvement of the thermo-oxidative resistance in high-temperature composites offers the potential to dramatically enhance the performance of the composite systems that are currently available. The reactive finish concept is shown schematically in Figure 1 where the finish chemically bonds to the fiber surface and to the polymer matrix to provide a well-bonded, durable interphase.

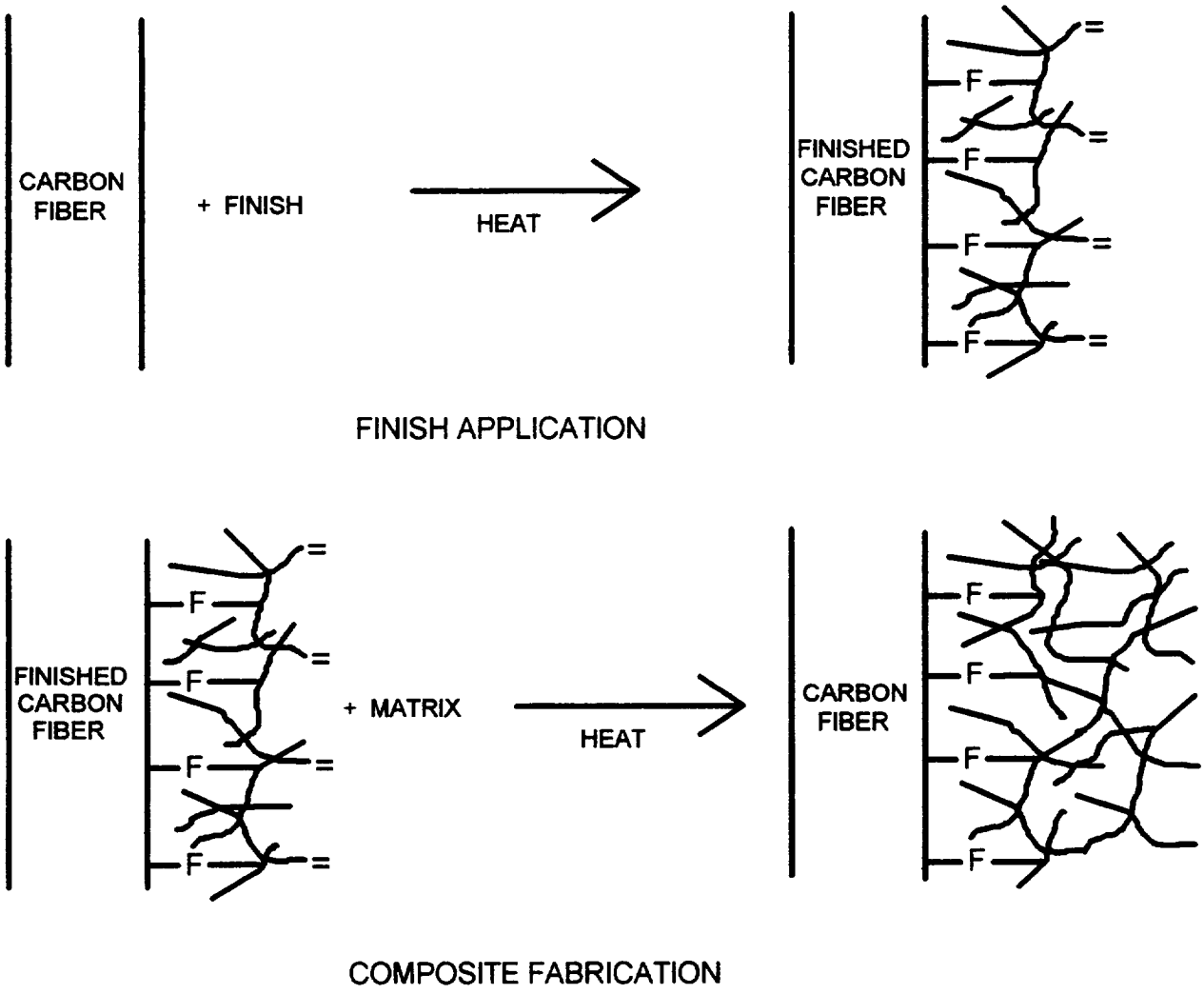

Figure 1. Reactive finish interfacial bonding concept

In this work, we distinguish a finish as an adhesion-promoting chemistry applied to a fiber surface from a sizing, which is applied as a handling aid. The reactive finishes are composed of four or more ingredients including a reactive coupling agent, a film forming polymer carrier, a surfactant, and a solvent. Mixtures of some of these ingredients are often necessary for solubility and processing reasons.

The objectives of this program were to improve the TOS of carbon fiber/PMR-II-50 polyimide matrix composites through the use of reactive finishes. These finishes are expected to improve TOS by forming covalent bonds at the fiber/matrix interface. Spectroscopic results on composites aged at high temperatures show that the reactive finishes provide superior oxidation resistance to the interface; however, aging at temperatures in the region of the matrix glass transition temperature (Tg) introduces other degradation mechanisms that preclude measuring quantitative mechanical properties. When optimized, use of these finishes should result in composites with longer lifetimes in high-temperature applications.

Experimental Procedures

Coupling Agent Synthesis and Characterization

The first step in the program was to synthesize additional quantities of reactive coupling agents using previously developed techniques. Figure 2 depicts the generic structure of the proprietary coupling agents. The synthesis was carried out with controlled laboratory conditions for five variations of the structure shown in Figure 2.

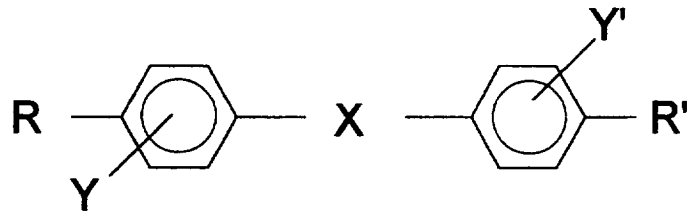

where X = linking group
Y, Y' = ring substituents
R, R' = proprietary functional groups.

Figure 2. Schematic chemical structure of reactive coupling agents

Verification of product purity was performed using a Mattson Cygnus 100 FTIR spectrophotometer. FTIR spectra were obtained on a sample of known purity and compared to the synthesized material. Thermal properties of the coupling agents were determined using a Perkin Elmer Series 7 differential scanning calorimeter (DSC) at a heating rate of 10°C/min. The synthesized coupling agents were shown

to be in excess of 97% purity by FTIR and were used as-produced for preparing the finish formulations.

Finish Formulation Development

Initial finish formulations using the five coupling agent variants contained 10 wt.% PMR-II-50 and 1 wt.% coupling agent in methanol. Ten percent polyimide proved to be too much and resulted in stiff impregnated bundles of fiber. Dilution of those solutions by a factor of 10 produced better handling finished fibers.

Bonding of the finish to the carbon fibers before prepregging is felt to be necessary so that the finish cannot be removed in the methanol solvent of the PMR-II-50 impregnation bath or diffuse into the matrix before bonding to the fiber. Attempts to bond the finishes to the carbon fibers using activation from ultraviolet (UV) light were unsuccessful. UV activation was considered attractive because it would reduce the potential for fires with any residual methanol. Thermal activation of the finish was successful with the set-up shown in Figure 3. Initial finish formulations for thermal activation used 0.1% coupling agent at 1.0 wt.% PMR-II-50 polyimide in methanol. Those formulations were applied to 3K T650-35 unsized carbon tows in the as-received condition.

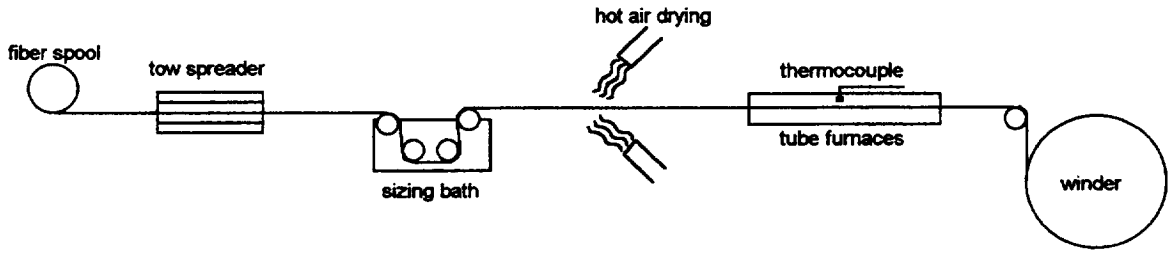

Figure 3. Schematic of finish application apparatus

A photograph of the finish processing line is given in Figure 4.

The set-up shown in Figures 3 and 4 is designed to spread the fiber tow allowing even coating of each fiber with the finish solution and drying before recollimating the tow so that fibers do not stick together. The drying step is accomplished with hot air blown over the fibers, which vaporizes most of the methanol and reduces the chance of a methanol fire in the tube furnaces. Temperatures in the tube furnaces were maintained at levels necessary to initiate the coupling reaction and imidization of the PMR-II-50 (200-225°C), but below those needed to cure the PMR-II-50.

Numerous formulations were prepared with the five reactive coupling agents. Formulation variables included concentrations of coupling agent and PMR-II-50 and solvent chemistry. Dip and spray coating of the finishes and cure temperature

were also evaluated in the set-up shown in Figures 3 and 4. In the spray process, the finishing bath was replaced with spray nozzles placed above and below the fiber tow. Problems were encountered with limited solubility of the finishes in methanol. Those problems were solved by using methanol/acetone blends. Finished fiber samples thought to be of good quality from appearance and feel (*i.e.*, not too stiff and without fibers stuck together) were selected for further evaluation.

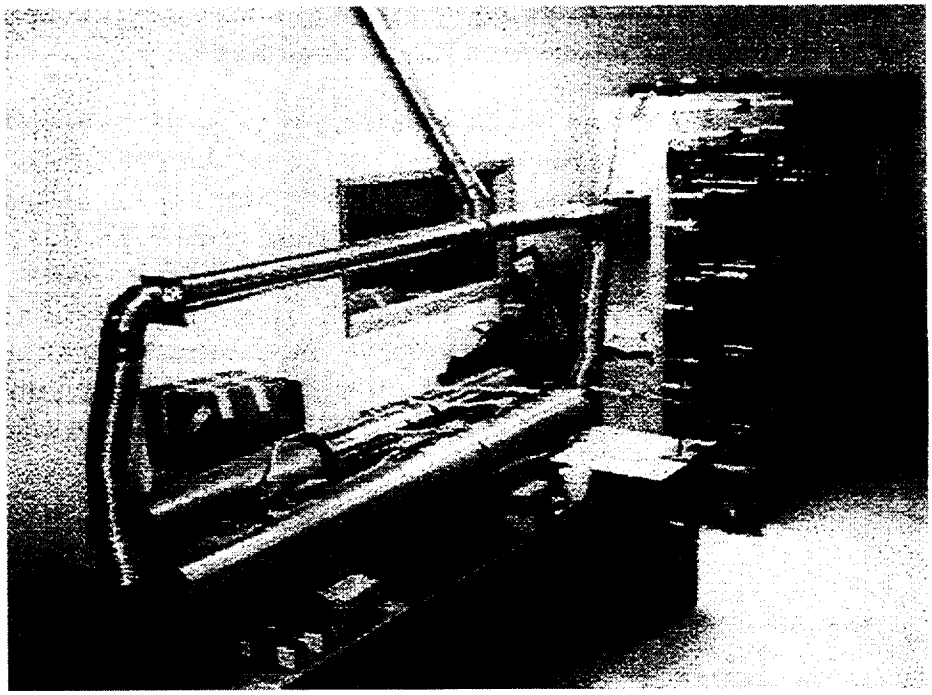

Figure 4. Finish processing line

The selected finished fiber sample lots were then divided in half. One-half was saved for scanning electron microscopy (SEM) evaluation in the as-finished condition. The other half of each lot was soaked in methanol at room temperature for two hours. The methanol soak was conducted to evaluate the fiber-finish bonding. Unbonded finish should be removed by the methanol wash. Sixteen methanol-soaked samples were then evaluated using SEM. Both application methods (spray and dip) coated the fibers uniformly and produced good grafted coatings at similar speeds. Because of its simplicity, the dip process was selected for use in the balance of the program.

To aid in the selection of the finish formulations to use in the composite aging studies, an additional screening test was used. The coupling agent-to-polyimide carrier ratio in the finish determines the mechanical properties (strength, stiffness, toughness) of the interphase region. Preparation of an interphase with moderate stiffness and toughness was attempted in this program. An initial feel for the finish mechanical properties was obtained by bending the fibers over a small radius

and observing for evidence of cracking. Single fibers were spirally wound around a small-diameter cylindrical core to investigate the integrity of the fiber coatings when subjected to small bending radii. Approximately 3-7 single fibers (filaments) were removed from a yarn and spirally wound around a 0.046-inch (1.18 mm) cylindrical core. The core was mounted to an aluminum stem with silver conductive paint. The specimens were sputter-coated with gold (Au) for 30 seconds at 50 mTorr and 40 mA using a Denton Vacuum DESK II Cold Sputter/Etch Unit to a thickness of approximately 100 angstroms. The fiber surfaces were analyzed and the mean fiber diameters were measured using an AMRAY 1830 scanning electron microscope at 20 keV.

Finish Characterization

To evaluate the thermal properties of bulk finish material, molding powders were fabricated with three finish formulations and neat PMR-II-50. The three finish powders were prepared using the same procedure. A solution of 2.5 g of coupling agent in methanol or acetone was added to 50 g of PMR-II-50 solution (50% solids) and mixed for 1 hour. The mixture was then heated for two hours at 50°C (122°F) to evaporate the solvents. The solid material was then heated to 170°C (338°F) and held for two hours to activate the coupling agent. After cooling to room temperature, the solid, foam-like material was ground to a fine powder and then reheated to 204°C (400°F) for two hours to imidize the PMR-II-50. The neat PMR-II-50 was processed in the same manner.

Molding of the powders into polymer disks was conducted at NASA LeRC using the following process. The powders were loaded into a cold die between Kapton release plies, heated to 316°C (600°F) where 2000 psi was applied in two bumps. After the second bump, the pressure was left at 2000 psi and the temperature raised to 371°C (700°F) and held for 15 minutes. The molded disks were then slow cooled to 204°C (400°F) where pressure was released and the part removed. After molding, the disks were postcured by heating to 288°C (550°F) in 1 hour, held 1 hour, heated to 316°C (600°F) over 1 hour and held 1 hour, heated to 343°C (650°F) over 2 hours and held 4 hours, heated to 371°C (700°F) over 2 hours and held 16 hours before cooling to room temperature over 3 hours. Thermal properties of the moldings were determined using thermal mechanical analysis (TMA) and thermogravimetric analysis (TGA) both at a heating rate of 10°C/min. The thermophysical properties of the finishes should be representative of the composite interphase properties.

Prepreg Fabrication

Initially, prepregs were manufactured by wet filament winding using a drum winder. This approach proved to have too much variation in resin content to produce consistent high-quality composite laminates by autoclave molding. The inconsistency in the prepregs caused considerable variation in the quality of

laminates used in the 400°C screening tests discussed in the Results and Discussion section. After the quality of those laminates was determined, the wet impregnation technique was abandoned.

Later prepregs were manufactured by drum winding the fiber dry followed by resin impregnation using a technique previously developed at NASA LeRC. Dry T650-35 fibers were first wound at a rate of 27 turns per cm to a width of 22.5 cm, which when cut yielded prepregs with dimensions of 22.5 x 60 cm. PMR-II-50 neat resin was applied at a rate of 100 g of 50 wt.% solution per winding as-received from Maverick Corp. (Cincinnati, OH). The resin was applied from solution using a brush. Prepregs were allowed to dry first in air and then by placing them in an oven at 75°C for 2-3 hours. After drying, the prepreg was pliable and had good drape characteristics. Prepreg weights were recorded to determine weight percent resin. Variations in fiber and resin content in the prepregs were within ± 2% from one prepreg to the next, demonstrating good reproducibility in prepreg manufacturing. Prepregs were then wrapped in polyethylene and aluminum foil and stored at -18°C until needed for the composite panel fabrication. Three types of prepreg were fabricated for this study: a control fiber using Amoco T650-35 3K 000 NT (unsized) and that same fiber finished with P9306F and P9307F.

Composite Processing

Initial unidirectional composites were fabricated in an autoclave using cure procedures based on platen press schedules previously developed by NASA LeRC. Eight-ply stacks of staged prepregs were used to fabricate the unidirectional composites for the thermal aging studies. The cure cycle entailed a rate ramp of 1.4°C (2.5°F) per minute to 371°C (700°F). At 316°C (600°F), a pressure of 290 psi was introduced. Pressure buildup was complete when the system reached 343°C (650°F). The composites were cured at 371°C (700°F) for 2 hours and then cooled at a rate of 1.44°C (2.6°F) per minute to 177°C (350°F). Final cool down to ambient was performed at a rate of 1.55°C (2.8°F) per minute. Full vacuum was maintained throughout the process. The molded composite panels had a final 0.20 cm (0.080 in.) thickness. The laminates were then subjected to a step postcure to a final 16-hour hold at 371°C (700°F) in flowing air.

Composite panels for the 400°C (752°F) screening tests and the 316°C (600°F) aging tests were produced using autoclave molding as described above. Panels for the 371°C (700°F) aging tests were produced at NASA LeRC using vacuum bag hot press molding with a similar cycle. The main difference between the molded panels was that the hot press molding was done at 500 psi applied pressure and the autoclave molding was done at 290 psi.

Composite Panel Characterization

Composite panels for the 400°C (752°F) screening tests were used as-produced. Laminate quality was confirmed with ultrasonic C-scan inspection, optical microscopy, and thermal analysis. Only materials with nominally less than 2% voids and representative Tgs were selected for mechanical testing. Ultrasonic nondestructive inspection was performed on the autoclaved composite panels using an Ultra Image IV system. Standard procedures developed for other composite systems were used for interpretation of the scans. Estimates of void content were obtained using image analysis of polished cross-sections.

Image analysis was performed on polished cross-sections of thermally aged test samples taken away from the fracture zone. The specimens were polished with 220 grit SiC, 6μ diamond, and 1μ diamond, cleaned ultrasonically, and inspected for defects at 400X magnification before imaging. Image analysis was performed on a Leitz MM6 microscope with direct bright field tungsten illumination. Images were captured on a Macintosh IIx computer containing a DT2255 QuickCapture frame grabber (Data Translation, Inc.) attached to a Sony XC-77 CCD TV camera on the microscope. Image analysis was accomplished using NIH Image 1.55 software. Magnification was 50X and frame resolution was 640 x 480.

TMA and TGA analyses were run on samples from the composite plates using a DuPont Instruments Model 943 at NASA LeRC with a heating rate of 10°C per minute. Tg was determined at the knee of the thermal expansion curve. Tgs were also determined with a Rheometrics RMS 800 using a torsion/rectangular configuration at a heating rate of 5°C per minute that verified the TMA results.

Thermal Aging

Before thermal aging, the composite panels were machined into 0.625 cm (0.25 in.) wide transverse (90°) flexure specimens, longitudinal (O°) flexure specimens, and short beam shear (SBS) specimens. The bars were rough cut with a diamond band saw, and finish machined to tolerances with a diamond end mill. After the specimens were machined, they were visually examined for defects and their edges polished with emery paper. All machined composite specimens were then dried in a laboratory oven at 100°C (212°F) for three days. The specimens were allowed to cool in a desiccator and were labeled with a permanent silver paint marker as well as with an engraving tool to ensure proper identification. Sample weights were taken using a five-place Mettler analytical balance.

Thermal aging was performed in a furnace that conformed to ASTM E-145 (Type IIA). The specimens were randomized in the oven. Stainless steel plates were placed on the specimens during thermo-oxidative aging to reduce warping. Aging was performed at three different temperatures: a 400°C (752°F) screening test and

was performed at three different temperatures: a 400°C (752°F) screening test and longer exposures at 371°C (700°F) and 316°C (600°F). Composite samples were removed from the desiccator and placed in the oven laying in a flat configuration on one of the oven's perforated shelves, to initiate the aging study. Specimen sets were removed periodically, cooled, weighed, desiccated, and tested. Despite the stainless steel plates placed on the specimens during aging, some warping was noted, particularly at the 400°C (752°F) aging temperature.

Mechanical Testing

Flexure testing on 0°, 90°, and SBS specimens at room temperature and at 288°C (550°F) was conducted in accordance with ASTM D-790. A 10:1 span-to-depth ratio was used for both flexure tests and a 4:1 ratio was used for the SBS tests in accordance with ASTM D-2344. Testing was performed at a rate of 0.02 cm/min.

Spectroscopic Characterization

Micro-FTIR techniques were used to identify chemical structural changes caused by thermo-oxidative exposure. Typical polymer-based material systems have very low IR reflectance values and hence are best analyzed by transmission or by internal or attenuated reflectance methods. Although standard FTIR microscopes can be used to characterize polymeric materials in reflectance, very large aperture sizes (100 x 100 μm) are needed to allow adequate signal throughput. At these aperture sizes, though, one obtains very little spectral discrimination between the different material components (resin, fiber) of the system. For microanalysis over areas of several microns, one typically prepares a thin section of the material using various microtome techniques. Microsectioning of carbon-fiber-reinforced polymer matrix composites, though, is quite difficult.

For these reasons, the utility of characterizing carbon/polyimide composite cross-sections using the enhanced sensitivity provided by an FTIR microscope integrated with a synchrotron light source at Brookhaven National Laboratory was investigated. The enhanced sensitivity provided by the High Brightness FTIR microscope eliminates the need for this microtome sectioning of composite specimens for IR micro-analysis over small areas. This new technique provides a simple and quick method for determining local variations in chemical structure in the composite system such as in damage gradients due to thermal aging. Procedures were developed that allowed high-resolution FTIR reflectance spectra to be obtained from carbon/polyimide composite cross-sections down to the diffraction limit of the microscope (5 x 5 μm aperture).

Several carbon/polyimide fiber composite cross-sections were prepared using standard mounting and polishing procedures. Micro-FTIR characterization was conducted on thermally aged specimens after mechanical testing.

Additional characterization was conducted on the transverse test specimens using VCXPS after the technique given in Ref. 5. The specimens were split to expose a fresh transverse surface and the ratio of carbon in the fiber (C_f) to carbon in the matrix (C_m) measured on a Fisons Escalab MKII instrument with 20 eV Mg kcc X-rays and a 5 x 2 mm spot size. The composite specimens were analyzed with respect to ground, ground plus an electron flood gun operated at 12 V and 1 mA, and with the flood gun and a +9 V battery bias voltage with respect to ground.

Results and Discussion

Coupling Agent Characterization

A sample DSC thermogram for the AT-CA-9306 coupling agent at a heating rate of 10°C/min is shown in Figure 5. The thermogram in Figure 5 shows the sharp endothermic melting of the crystalline coupling agent at 44°C (111°F) followed by a wide ranging decomposition exotherm beginning at 131°C (268°F) continuing to 200°C (392°F).

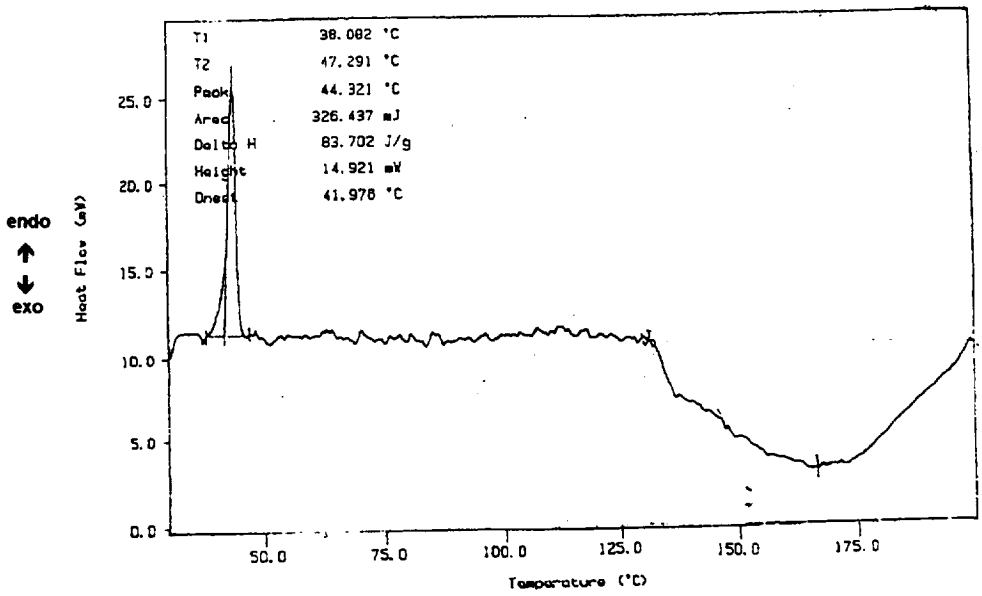

Figure 5. DSC thermogram at 10°C/minute for the AT-CA-9306 reactive coupling agent

Similar features are seen in the DSC thermograms for all the coupling agents. A summary of the coupling agent DSC results is given in Table I. The DSC data describes the melting point (T_m) and decomposition temperature (T_d) range for the bonding reaction for each reactive coupling agent.

Table I. DSC Characterization Results for Reactive Coupling Agents at a Heating Rate of 10°C per Minute

Coupling Agent	T_m (°C)	ΔH_{melt} (J/g)	T_d onset (°C)	T_d max (°C)	T_d end (°C)	ΔH_d (J/g)
AT-CA-9301	*	--	135	170	**	- 881
AT-CA-9304	137	52.8	138	144	163	-528
AT-CA-9306	44	83.7	131	165	200	-859
AT-CA-9307	74	120.6	149	186	203	-976

*Not evident.
**Peak 2 onset 185, max 196, end 215.

The coupling agents display a wide range of melting points, reaction onset temperatures, and maximum reaction temperatures. That variability allows finishes to be tailored to the desired cure cycle for the composite.

Finish Development

Numerous coating trials were conducted for applying the reactive finish using the set-up shown in Figures 3 and 4. The purpose of these trials was to determine the effects of application method and finish concentration on the final finish uniformity, thickness, and subsequent reactivity with the carbon fiber surface. Results of the finishing trials are given in Table II. The AT-CA-9307 coupling agent was added to the test matrix later and is not included in the Table II results. Subsequent tests with the AT-CA-9307 in the PMR-II-50 finish showed that it displayed the same behavior as the other finishing systems.

The diameter results given in Table II show that the finishes vary from 0.15-0.75 μ (5.9-29.5 x 10^{-6} in.) in thickness with the majority near 0.5 μ (19.7 x 10^{-6} in.). The finish uniformly coats the fibers without adhering fibers together. This shows that the PMR-II-50 polyimide is a good film former for use as the finish base. For the most part, little of the finish is removed by a methanol wash, which shows that the processing conditions studied are adequate to initiate the coupling reaction and that the desired bonding is taking place. After finishing, the tow has excellent handleability for subsequent processing. Photomicrographs of unsized T650-35 carbon fibers with applied finish and after methanol extraction are given in Figures 6-8.

Table II. Characterization Results for Sized Fibers

Coating	Solvent	Coating Method	Feed Rate (cm/sec)	Cure Temp. (°C)	Rinse	Fiber Diameter (μm)
None (unsized T650-35)	--	--	--	--	--	6.8*
0.01% AT-CA-9301, 1% PMR II-50	MeOH	Spray	16.5	150	--	7.85
0.01% AT-CA-9301, 1% PMR-II-50	MeOH	Dip	16.5	150	--	8.3
0.01% AT-CA-9301, 1% PMR-II-50	MeOH	Dip	16.5	150	MeOH	8.05
0.01% AT-CA-9301, 1% PMR-II-50	MeOH	Spray	16.5	150	MeOH	8.1
1% AT-CA-9304, 1% PMR-II-50	MeOH	Dip	16.5	170	MeOH	7.1
1% AT-CA-9304, 1% PMR-II-50	MeOH	Dip	16.5	170	--	7.07
0.05% AT-CA-9304 1% PMR-II-50	Mixed	Dip	16.5	175	--	8.3
0.05% AT-CA-9304, 1% PMR-II-50	Mixed	Dip	16.5	175	MeOH	7.8
0.1% AT-CA-9301, 1% PMR-II-50	Mixed	Dip	16.5	175	--	8.1
0.1% AT-CA-9301, 1% PMR-II-50	Mixed	Dip	16.5	175	MeOH	7.95
0.1% AT-CA-9306, 1% PMR-II-50	Mixed	Dip	16.5	175	--	8.0
0.1% AT-CA-9306, 1% PMR-II-50	Mixed	Dip	16.5	175	MeOH	7.1
0.01% AT-CA-9306, 1% PMR-II-50	Mixed	Dip	40	175	--	7.6
0.01% AT-CA-9306, 1% PMR-II-50	Mixed	Dip	5	175	--	7.4
0.01% AT-CA-9306, 1% PMR-II-50	Mixed	Dip	40	175	MeOH	8.1
0.01% AT-CA-9306, 1% PMR-II-50	Mixed	Dip	5	175	MeOH	7.5

*Amoco Product Literature.

Figure 6. Appearance of unsized T650-35 carbon fiber surface

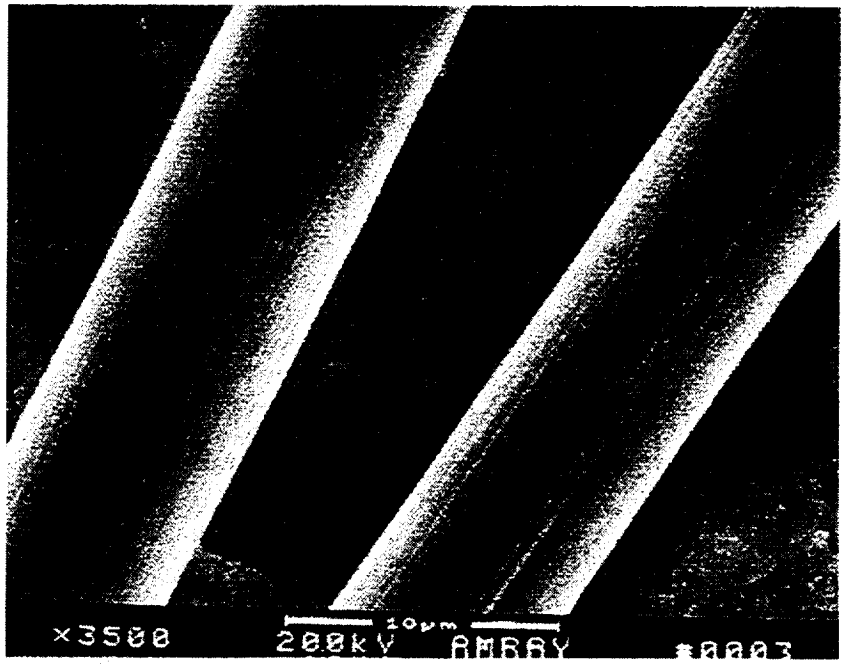

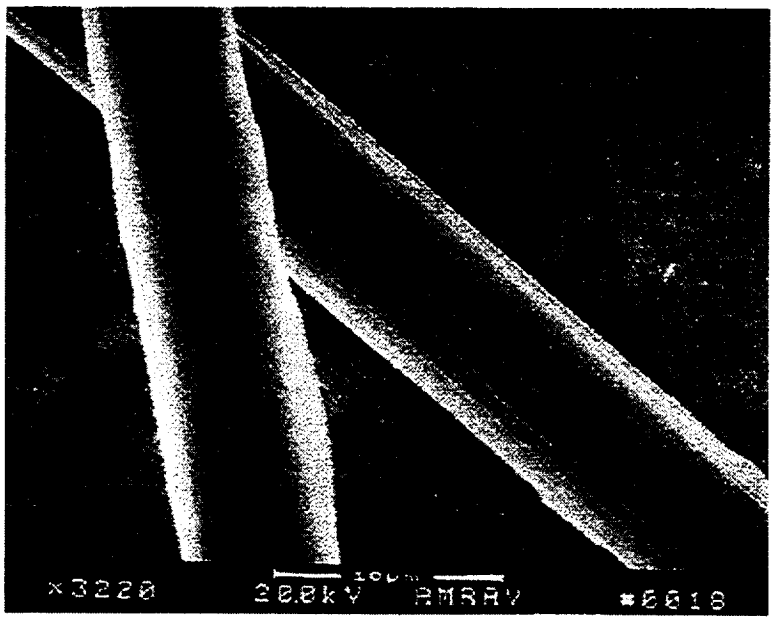

Figure 7. Appearance of finished T650-35 carbon fiber surface

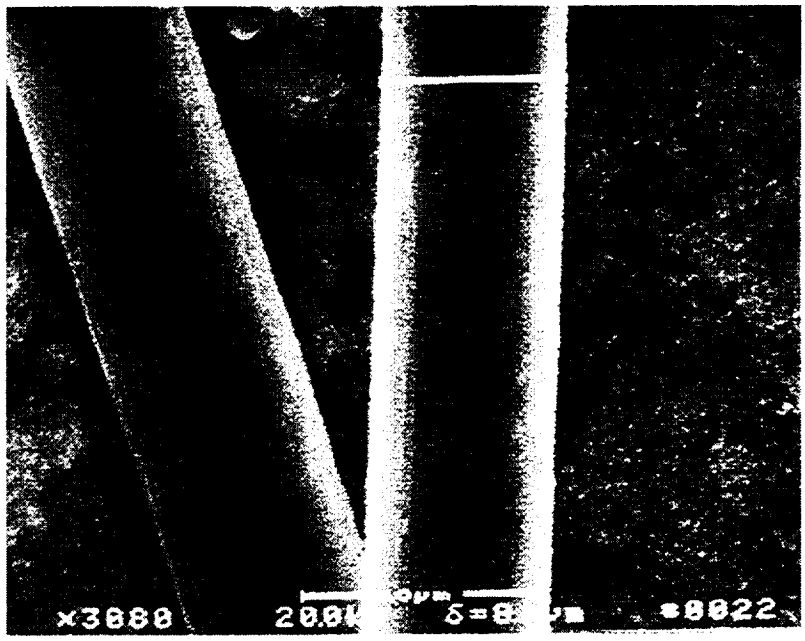

Figure 8. Appearance of finished T650-35 carbon fiber surface after methanol wash

The finished fibers seen in Figure 7 are generally smooth indicating that the finish has filled in the striations evident on the unsized fibers shown in Figure 6. After methanol wash (Figure 8), the finish appears rougher than the as-fabricated texture. The roughening is likely due to the removal of unbonded PMR-II-50 carrier. When fabricated into a fully-cured composite, that PMR-II-50 would be bonded into the matrix network and become part of a sound interphase region.

SEM observations of finished fibers bent over a 1-mm diameter radius showed no evidence of cracking at coupling agent concentrations up to 1%. This shows that the coupling agent is not embrittling the finish, which could form an undesirable interphase structure. A representative finished fiber surface formed to a 1 mm diameter radius is shown in Figure 9.

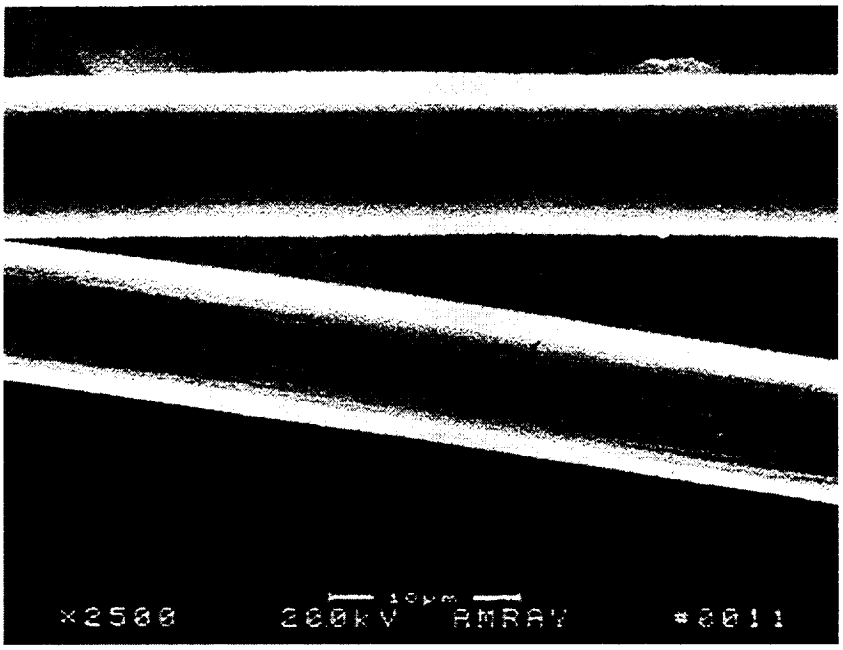

Figure 9. Appearance of finished T650-35 fibers after methanol extraction and bending over 1 mm radius

The SEM observations are very encouraging. In general, the finishes uniformly coated the fiber. All of the finished samples showed evidence of a coating adhering to the fibers even after the two-hour methanol wash, and little polymer was seen in the wash solution. This implies that all of the coupling agents reacted to form covalent bonds between the fibers and PMR-II-50 carrier. Subsequent incorporation of the fibers with grafted PMR-II-50 into a PMR-II-50 matrix composite should result in a more oxidation-resistant material. Based on these results, finishes were applied as 1.0% solutions with 0.1% reactive coupling agent for the majority of the thermal aging studies.

Finish Characterization

A plot of the cure behavior of PMR-II-50 at a 10°C (50°F) heating rate is given in Figure 10. The polyimide shows little thermal activity before the beginning of a large curing endotherm beginning near 200°C (392°F).

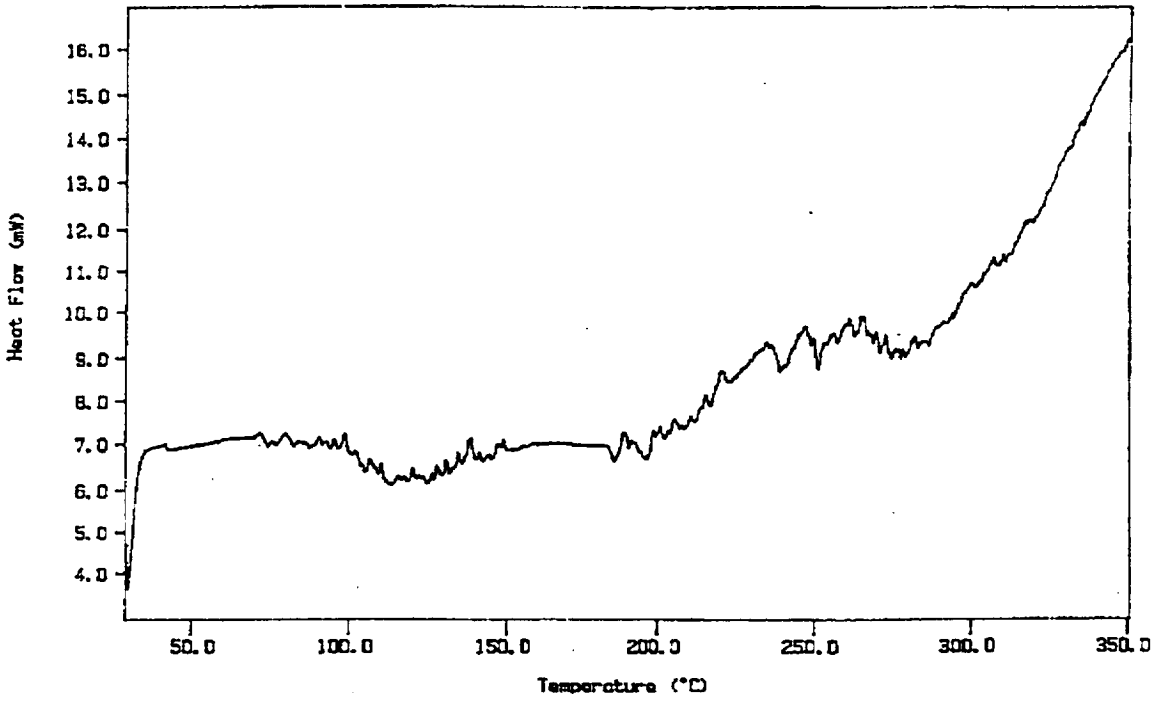

Figure 10. DSC thermogram at 10°C/minute for PMR-II-50 resin

Similar DSC thermograms were obtained on dried finish formulations. A representative thermogram for the P9306F finish is shown in Figure 11.

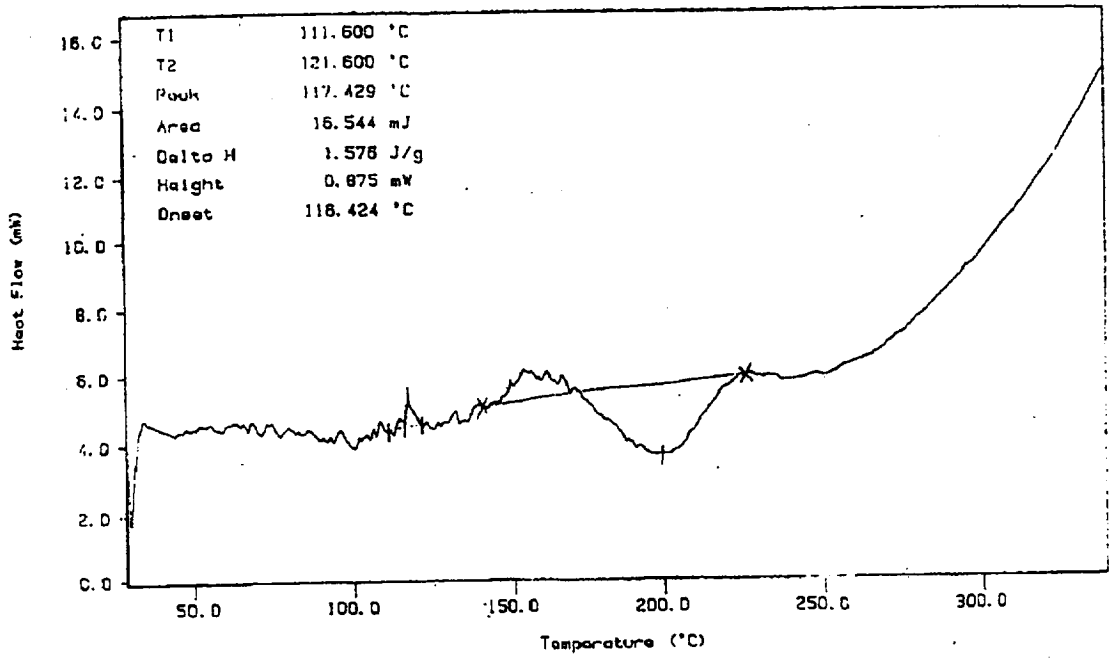

Figure 11. DSC thermogram at 10°C/minute for P9306F finish

Examination of the finish thermograms reveals the following observations. Melting points seen for the coupling agents are not evident in the finish mixtures. This shows that the coupling agents are molecularly dispersed in the mixtures and do not exist as islands of crystalline material, which would be detrimental to performance. All the finish thermograms show an endotherm beginning around 150°C (302°F) (Figure 11). This is not seen in any of the individual plots for PMR-II-50 or the coupling agents. The small endotherm at 150°C is likely due to the evolution of residual methanol solvent that was hydrogen bonded into the polymer. That endotherm is overcome by the large exotherm from the coupling agent decomposition in all cases before the polyimide curing endotherm becomes the dominant feature at high temperatures.

TGA results for the molded finish compositions are given in Table III. The thermal characterization results given in Table III show that the finish formulations generally have a higher Tg than the neat PMR-II-50 and display a slightly lower degradation onset temperature in air or in nitrogen.

Table III. Thermal Analysis Results for Neat Molded Finish Compositions at a Heating Rate of 10°C Per Minute

Finish	Tg before postcure (°C)	Degradation Onset air/N_2, before postcure (°C)	Tg postcured, (°C)	Degradation Onset air/N_2, postcured (°C)
PMR-II-50	319	527/503	355	538/515
P9304F	332	519/494	354	530/518
P9306F	289	510/493	379	513/507
P9307F	296	506/503	391	516/507

The higher Tg of the finish is consistent with the expected higher cross-link density from reaction of the coupling agent and the polyimide carrier. The thermal degradation results seem to show that the finish has a slightly lower thermal stability than the neat polyimide; however, its thermal stability is close enough to that of the PMR-II-50 to provide good TOS in carbon fiber-reinforced composites.

Thermal Aging

Three separate thermal aging studies were conducted during the program. Initially, an accelerated aging study was conducted for short times at 400°C (752°F). Long-term aging studies were then conducted at 371°C (700°F) and 316°C (600°F). In

each study, the mechanical properties of the aged composites were determined and the specimens thoroughly characterized using spectroscopic techniques.

400°C Screening Tests

The first set of composite laminates produced in the program by autoclave molding was used to screen the various finishes for composite TOS using transverse flexure specimens aged at 400°C (752°F). Room temperature transverse flexure results for as-fabricated and thermally aged (16 hours, 400°C in air) composite specimens are given in Table IV.

Table IV. Transverse Strength Results for T650-35/PMR-II-50 Composites

Sample	As-Fabricated MPa (ksi)	Coefficient of Variation (%)	400°C Exposed MPa (ksi)	Coefficient of Variation (%)	Loss (%)
Unsized Control, Set 1	126.9 ± 13.8* (18.4 ± 2.0)	11	65.8 ± 1.9 (9.6 ± 0.3)	3	48
Unsized Control, Set 2	93.7 ± 25.1 (13.6 ± 3.6)	27	43.4 ± 15.7 (6.3 ± 2.3)	36	54
P9307F	129.5 ± 22.1 (18.8 ± 3.2)	17	118.4 ± 17.2 (17.2 ± 2.5)	15	8
P9306F Set 1	156.9 ± 6.8 (22.8 ± 1.0)	4	91.5 ± 2.4 (13.3 ± 0.4)	3	42
P9306F Set 2	140.8 ± 25.3 (20.4 ± 3.7)	18	56.0 ± 17.3 (8.1 ± 2.5)	31	60
P9306F Set 3, 0.01%	66.2 ± 13.6 (9.6 ± 2.0)	20	48.2 ± 11.6 (7.0 ± 1.7)	24	27
P9304F	61.4 ± 14.2 (8.9 ± 2.1)	23	53.9 ± 20.2 (7.8 ± 2.9)	37	12
P9301F	51.5 ± 11.5 (7.5 ± 1.7)	22	34.0 ± 5.2 (4.9 ± 0.8)	15	34

*Standard deviation.

In this initial study, composites were fabricated from prepregs produced with a simple wet winding procedure. Unfortunately, variations in the uniformity of the prepreg resulted in composite laminates with little control of fiber volume fraction.

Examination of the transverse flexure screening data given in Table IV shows that many of the panels used were not of sufficient quality due to high porosity, which may mask some of the results from the different finishes. Only specimen sets with as-fabricated strengths above 125 MPa are considered representative. The data sets below that range have high void contents from poor consolidation due to nonuniformity in the prepregs. The as-fabricated coefficients of variation are all similar even for the specimens with high void content. The strength loss values compared to the as-fabricated strengths may have meaning, but it is difficult to determine. Strength retention from porous samples may be an even more severe test. If we assume that the loss data from these screening tests is meaningful, then all of the finishes show better TOS than the unsized control with the exception of the P9306F Set 2. This indicates that the proposed interfacial bonding mechanism is occurring.

The best control (unsized) set lost 48% of its transverse strength after the thermal exposure while the P9307F finished sample set lost only 8% of transverse strength. The P9304F samples also showed good strength retention on material with high porosity that may have resulted in a more severe exposure. The substantial improvement in TOS seen with the P9307F finish led to a significant amount of characterization in an effort to understand the mechanism for the observed behavior. SEM, micro-FTIR, VCXPS, and DMA results are discussed below.

SEM analyses of the fracture surfaces of the transverse flexure specimens provide evidence of thermo-oxidative degradation in the unsized specimens exposed at 400°C (752°F) in air for 16 hours. The fracture surface topography in areas close to the specimen surface appears to be smoother with less evidence of resin fracture (*i.e.*, hackles and river markings) compared to the fracture surface in the center of these specimens. The center section of the exposed unsized specimens had a topography that was similar to that of unexposed, unsized specimens. Fracture surfaces from all areas of the P9307F finished specimens that were unexposed or exposed were similar to the as-processed unsized specimens. This difference in topography is consistent with the observed differences in post-exposure retention of strength in this sample set.

Micro-FTIR analyses supported the mechanical property results and SEM analyses. Spectra were obtained on polished surfaces of unsized and finished specimens prepared before and after thermal exposure. The micro-FTIR spectra were taken on the specimen ends (fiber ends exposed) near the outer surface and in the center of the specimen. The spectra showed that surface regions in exposed, unsized specimens underwent a change in chemistry that was reflected as a change in peak

height for a peak near 1300 cm^{-1}. Spectra taken from the center regions of these specimens were identical to those of the unexposed specimens. Spectra taken from all regions of the exposed, P9307F finished specimens were identical to those obtained from the unexposed specimens. Thus, there appears to be a difference in the TOS of the materials examined that is related to the presence of the reactive coupling agent-based finish.

Figure 12 shows the spectra of an unfinished control specimen near the outer surface as a function of aging time at 400°C (752°F). Results given in Figure 12 show that bands near 1150 cm^{-1} and between 1250 and 1300 cm^{-1} show considerable change as a function of increasing aging time. An enlarged view of that region is given in Figure 13. Analysis of these data concludes that the shoulder at 1260 cm^{-1} emerging on the sharp peak at 1250 cm^{-1} is due to a strained epoxy ring on an aromatic ring. Its location indicates that the aromatic structure is the carbon basal plane. Likewise, the disappearance of the peaks at 1516 cm^{-1} and 1210 cm^{-1} in Figure 12 is due to oxidation of the fiber surface. There is much less loss in those peaks in the finished material given in Figure 14. This is evidence of oxygen diffusing along fibers in the unsized material that does not occur in the finished material. Thus, these peaks provide a direct monitor of oxidation of the carbon fiber surface that results in delamination. The peaks disappearing near 1150 cm^{-1} and 720 cm^{-1} are perhaps due to a defluorination reaction in the PMR-II-50 evolving CF_3H, although they may also result from loss of aromatic C-H bonds through oxidation and coupling. Those peaks show less degradation in the finished material given in Figure 14. Likewise, spectra for the unfinished and finished composites taken near the center of the specimen where little oxidation would be expected for these aging times do not show the changes discussed above.

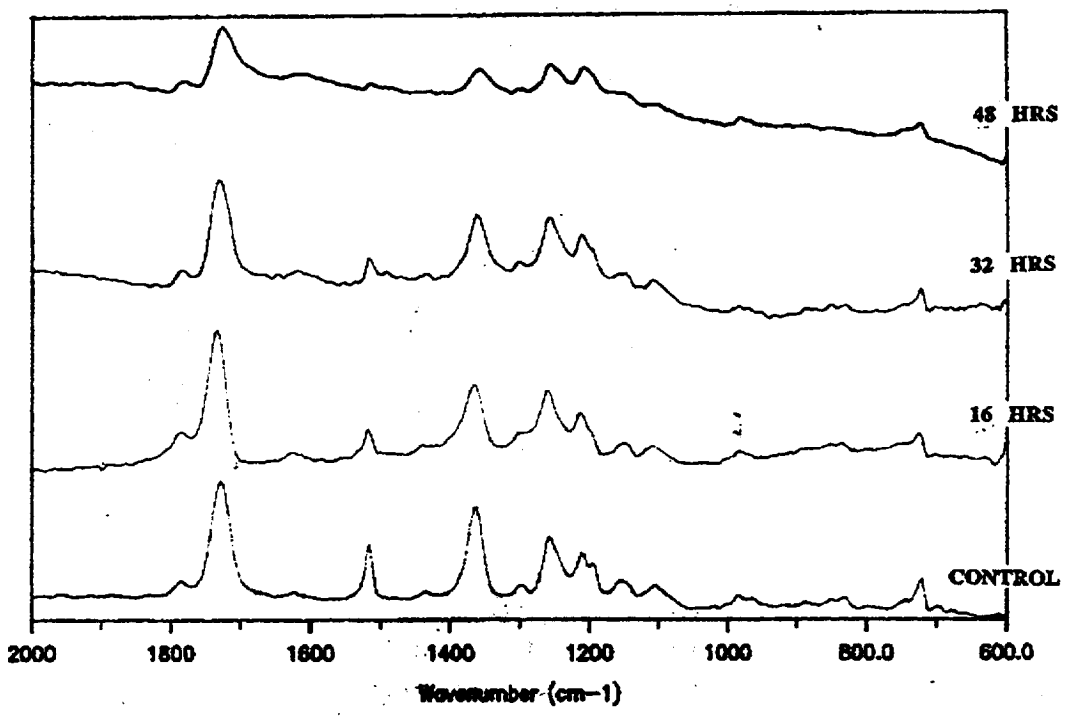

Figure 12. Micro-FTIR spectra of unsized control material near surface vs aging time at 400°C

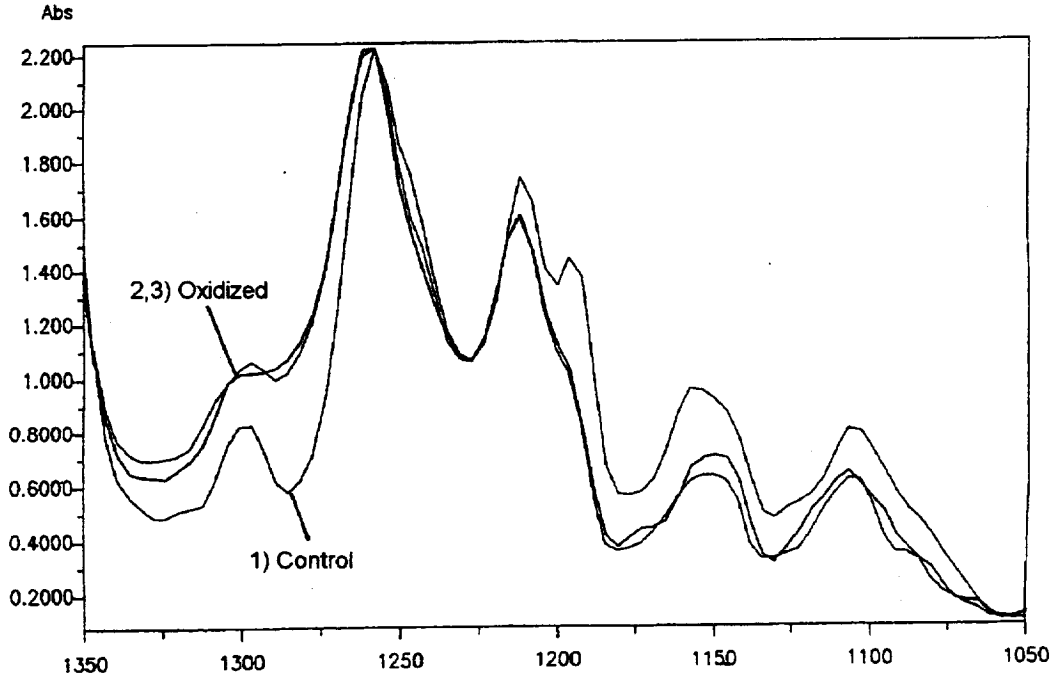

Figure 13. Enlargement of micro-FTIR spectra in 1200 cm^{-1} region

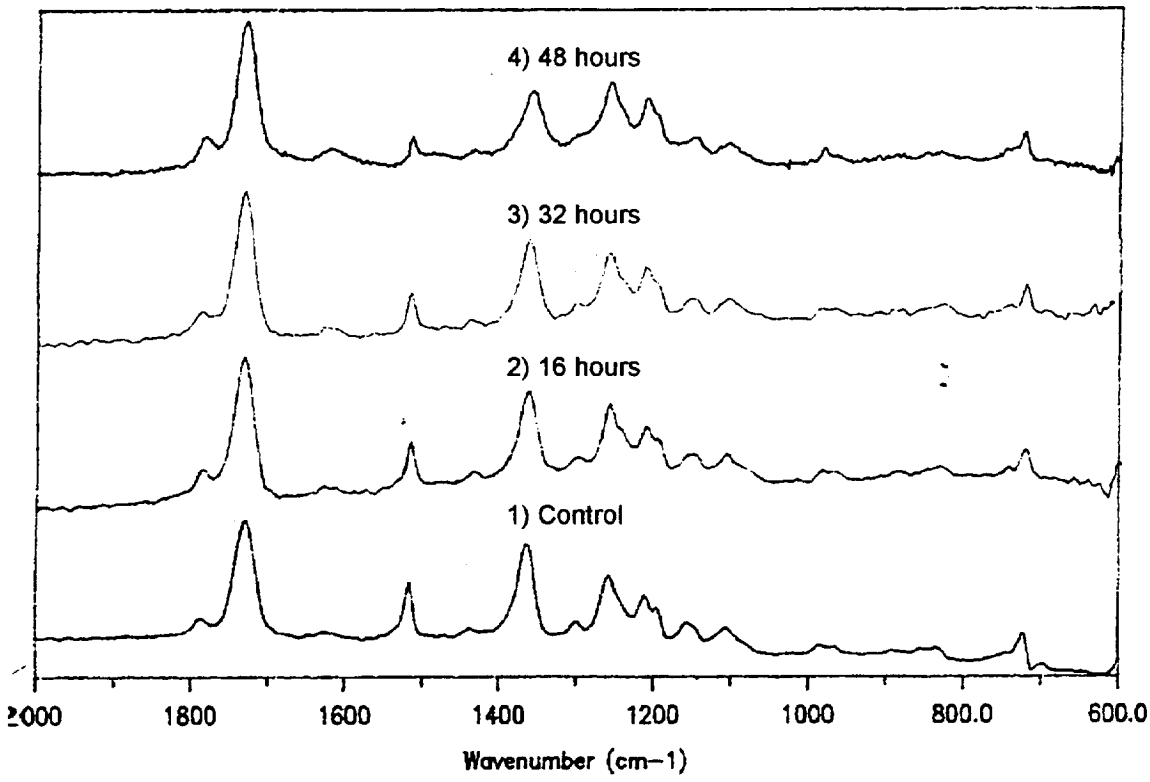

Figure 14. Micro-FTIR spectra of P9307F finished material near surface vs aging time at 400°C

VCXPS was run on the outer surface regions of selected samples from the accelerated aging study. VCXPS provides a means to quantitatively measure the amount of carbon fiber exposed on a transverse fracture surface. The ratio of fracture surface from carbon fiber to that from the polymer matrix is an indication of interfacial adhesion in the composite. A sample VCXPS spectra for the P9307F finished laminate C_{1s} region is shown in Figure 15.

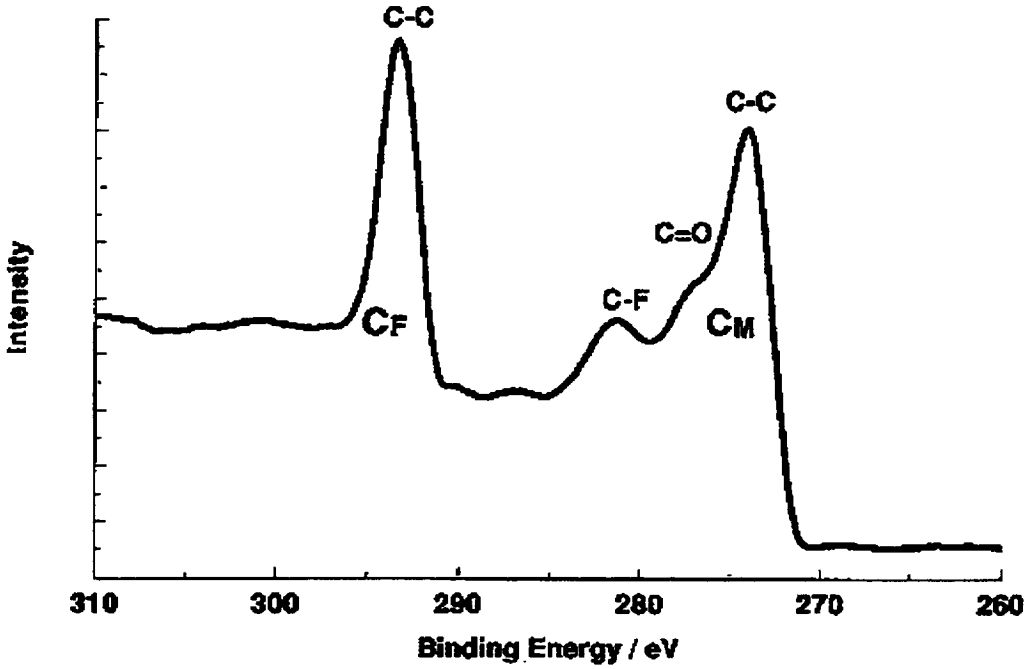

Figure 15. VCXPS for P9307F finished laminate fracture surface

In Figure 15, it can be seen that, with the applied +9 V bias, the two peaks from carbon fiber and PMR-II-50 are well separated and can be integrated accurately. A summary of the VCXPS results is given in Table V.

Table V. VCXPS Results for 16-hour 400°C Aged T650-35/PMR-II-50 Specimens

	As Fabricated (C_f/C_m)	Exposed (C_f/C_m)
Unsized Control	0.30 ± 0.03	0.42 ± 0.01
P9306F, Set 1	0.23 ± 0.04	1.38 ± 0.41
P9307F	0.28 ± 0.07	0.11 ± 0.01

Using the subjective scale of Miller *et al.* [5], the P9307F finished sample displays excellent interfacial adhesion after aging and the unsized sample displays good interfacial adhesion. The change in the VCXPS data for the P9306F finish does not correlate with the mechanical data given in Table V and cannot be explained without further testing.

Rheometrics DMAs were also performed to compare the Tgs and loss behavior of the P9307F finished composite to the unsized composite system. Testing was performed in the as-processed condition as well as after exposure at 400°C (752°F) for 16 hours. The DMA results are consistent with the chemical and mechanical property changes that have been discussed above. The thermo-oxidative exposure increased Tg and broadened the transition temperature range in the PMR-II-50 composites examined. Comparison of the P9307F finished composites (Figure 16) to the unsized control samples (Figure 17) shows that the finished materials have a considerably smaller change in Tg (approximately 20°C *versus* 60°C) and also show less broadening in the glass transition region. Thus, the finish appears to improve the environmental stability of the composite, and this translates into improved retention of composite properties after exposure.

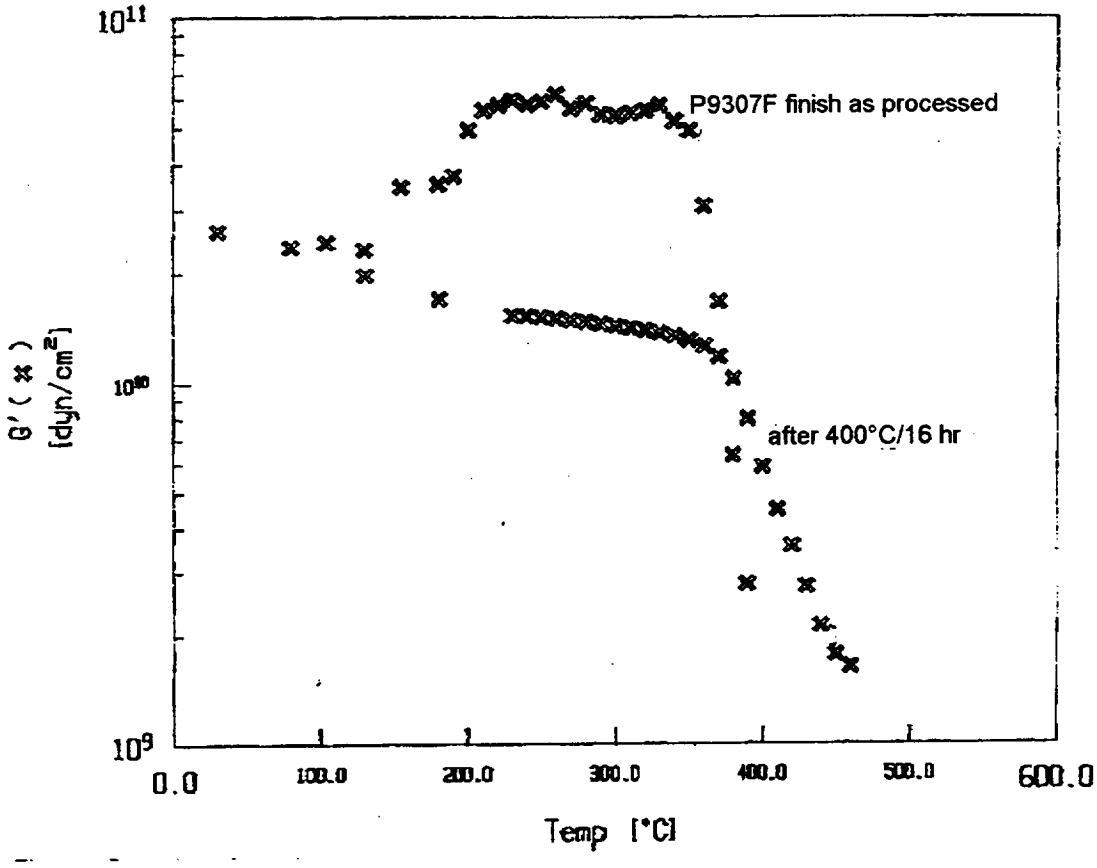

Figure 16. DMA plot for P9307F finished laminate after 16-hour 400°C exposure

Taken together, the results from the 400°C accelerated aging tests show that the finish may be inhibiting the oxidation reaction that is occurring at the carbon fiber surface in the unfinished composite. If this conclusion holds, these reactive finishes should have the potential to substantially improve the TOS of high-temperature composite systems. The P9307F finish showed clear promise for meeting the

program objectives and was selected for use in the balance of the program. The P9306F finish was also carried into the 371°C (700°F) aging studies.

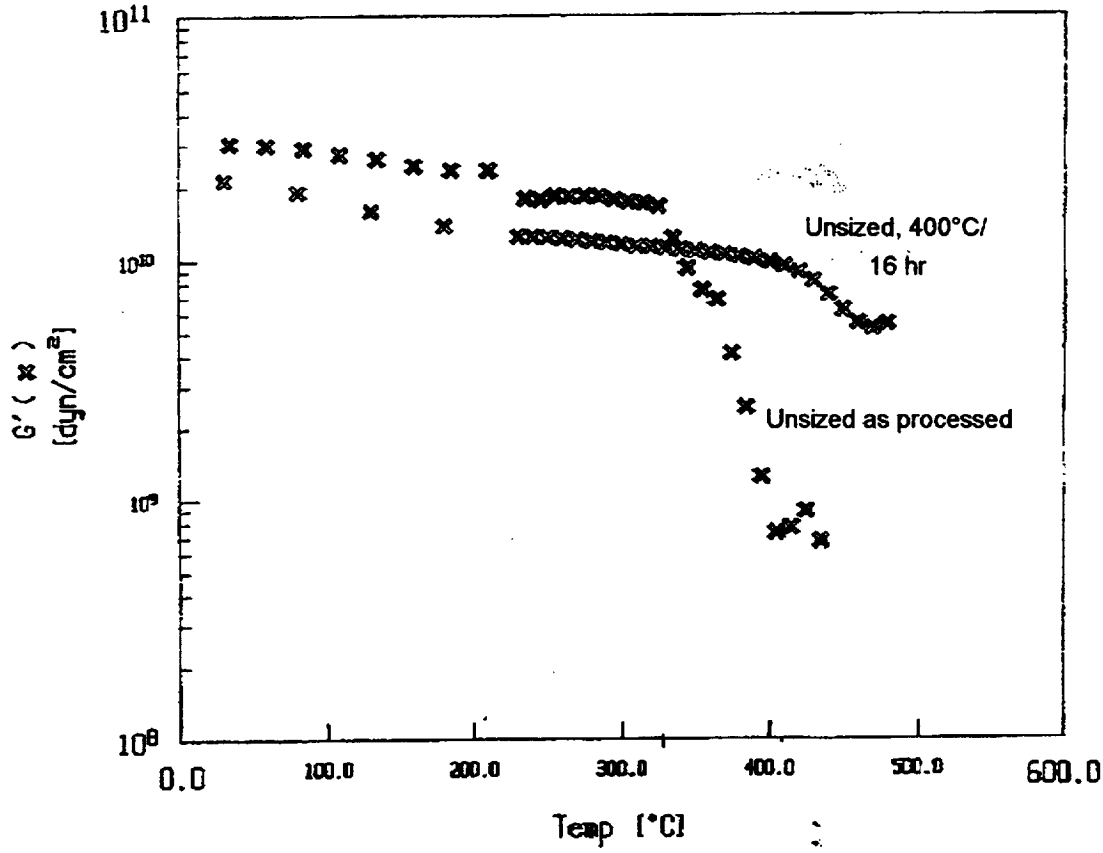

Figure 17. DMA plot for unsized laminate after 16-hour 400°C exposure

371°C Aging Study

Following the 400°C (752°F) screening tests, a larger accelerated aging study was performed at 371°C (700°F). Since the intent of the work was to quickly identify benefits achieved from the finishes, the aging conditions used were severe both in the temperature used and the high surface area-to-volume ratios in the specimens. Additional composite plates were fabricated using a vacuum bag hot press molding technique at NASA LeRC and thoroughly characterized using ultrasonic inspection techniques. Composite laminate quality was notably better than in the earlier 400°C (752°F) aging study. The unidirectional T650-35/PMR-II-50 composite plates that passed the nondestructive evaluations were then tested for thermal properties before being used in the thermal aging studies. A summary of the TGA and TMA composite results is given in Table VI.

Table VI. Thermal Properties of Composite Test Samples

Finish Type	Degradation Onset Air/N_2 before Postcure*	Degradation Onset Air/N_2 after Postcure*	Tg (TMA) before/after Postcure**	Weight Loss after Postcure (%)
Unsized Control	521/510	525/521	337/350	0.43
P9306F	504/519	528/515	317/337	0.47
P9307F	509/520	522/516	331/347	0.49

*TGA ramp rate = 10°C/min; values = °C.
**TMA ramp rate = 10°C/min; 5 gram weight with an expansion probe, values = °C.

The lower degradation onset temperatures seen for the bulk finish is not seen in the composite results given in Table VI. The thermal properties of all three composites after postcure are virtually identical. The unsized composite appears slightly less thermally stable than the bulk resin. Interestingly, the finished composites show a slightly higher resistance to thermal degradation than the bulk finishes. This may mean that the hypothesized interfacial reaction is increasing the thermal stability of the interface, which will result in a higher TOS composite. Composite Tgs of the finished material are similar to that of the unsized control sample. This means that the accelerated thermal aging at 371°C (700°F) performed in this phase of the work was at 20°C or more above the matrix Tgs.

After high-quality composites could be made from the dry-wound prepregging technique, mechanical properties were determined. Room-temperature test results for longitudinal and transverse flexure and SBS tests are given in Table VII. Longitudinal tests at 288°C (550°F) are also given in Table VII. The results given in Table VII show that the finished and unsized laminates have nearly equivalent properties in the as-fabricated condition. Longitudinal flexural strengths agree with literature values while the interface-dominated modes show higher values than previously reported for this material [24]. Transverse strengths agree well with the previous data sets given in Table IV for the 400°C (752°F) screening test control specimens. The P9307F finished material shows somewhat lower 0° flexural strength at room temperature and better strength retention at the 288°C (550°F) test temperature, which is indicative of a better bonded laminate. Transverse fracture surface appearance of all the materials was similar and displayed predominant cohesive failure (Figures 18 and 19).

Table VII. As-Fabricated Mechanical Properties of T650-35/PMR-II-50 Unidirectional Laminates

Surface Treatment	90° Flexure MPa (ksi)	Short-Beam Shear MPa (ksi)	0° Flexure MPa (ksi)	288°C 0° Flexure MPa (ksi)
Unsized Control	118.6 ± 9.0 (17.2 ± 1.3)	114.5 ± 1.1 (16.6 ± 0.6)	1,460.7 ± 104.1 (211.8 ± 15.1)	789.7 ± 6.9 (114.5 ± 1.0)
P9306F	114.5 ± 2.8 (16.6 ± 0.4)	107.6 ± 2.8 (15.6 ± 0.4)	1,428.3 ± 19.3 (207.1 ± 2.8)	717.3 (104.0)
P9307F	125.5 ± 6.9 (18.2 ± 1.0)	118.6 ± 0.7 (17.2 ± 0.1)	1,252.5 ± 72.4 (181.6 ± 10.5)	862.8 ± 148.3 (125.1 ± 21.5)

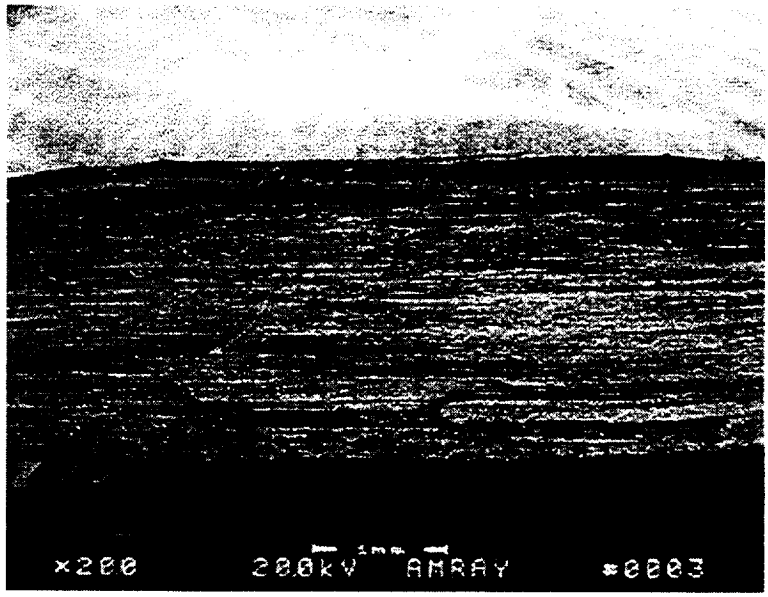

Figure 18. Transverse fracture surface of as-fabricated unsized T650-35/PMR-II-50 unidirectional laminate

The original intent of the program was to obtain long-term aging data on composite samples at 371°C (700°F) with and without the reactive finishes. To meet that objective, specimens from the high-quality plates used to generate the data in Table VII were aged for 16, 150, 331, and 700 hours before testing.

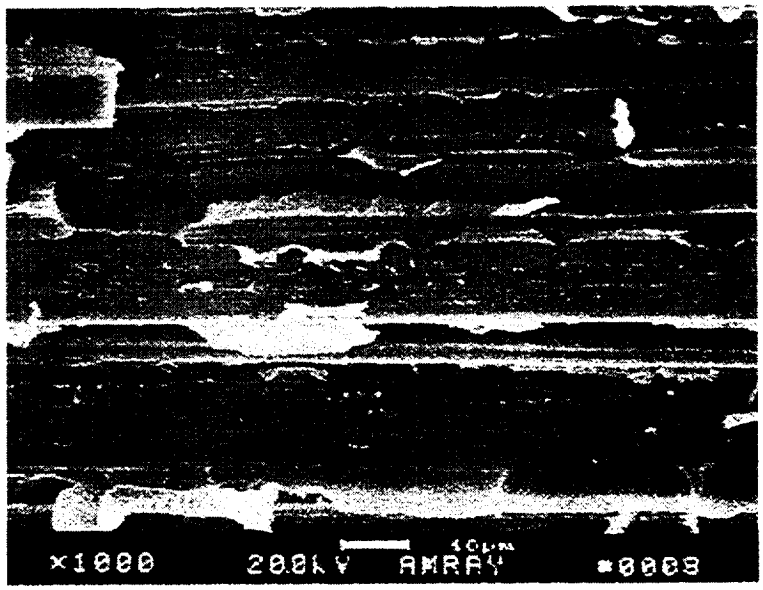

Figure 19. Magnified view of Figure 18 material showing matrix cohesive failure

Weight loss after 371°C (700°F) aging in air is given in Figures 20 and 21 for 0° and 90° flexure specimens. As indicated, extensive degradation was observed in all cases at modest exposure times. The data given in Figures 20 and 21 show that the finish improved the TOS of the 90° flexure specimens. These specimens should be dominated by interfacial attack, whereas the 0° specimens that have fewer exposed fiber ends per unit volume of sample should be dominated by bulk degradation. Bulk degradation at long exposures could be expected to obscure any potential benefit from improved interfaces.

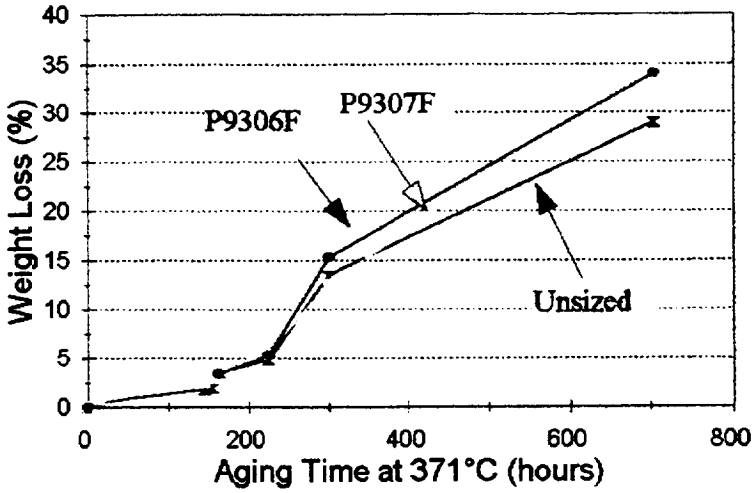

Figure 20. Weight loss as a function of aging time at 371°C (700°F) for 0° flexure specimens

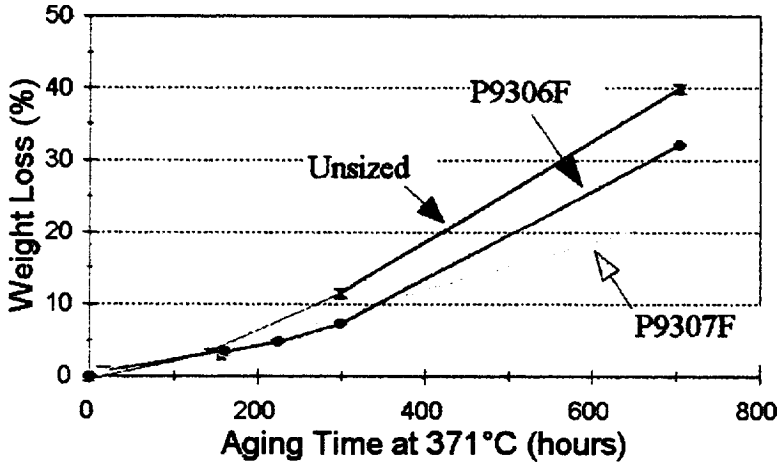

Figure 21. Weight loss as a function of aging time at 371°C for 90° flexure specimens

Results for longitudinal and transverse flexure strength of T650-35/PMR-II-50 composites as a function of aging time are shown in Figures 22 and 23. These results show that the finish does reduce the kinetics of oxidation initially. They also show more strength loss in the transverse specimens after 16 hours of aging, which is expected because of the high number of exposed fiber ends in the gauge section of the specimens.

Figure 22. 0° flexural strength retention of T650-35/PMR-II-50 laminates

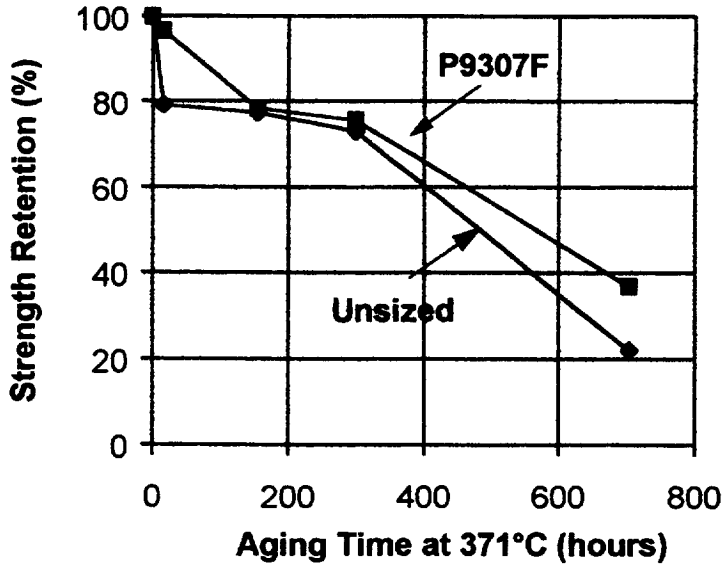

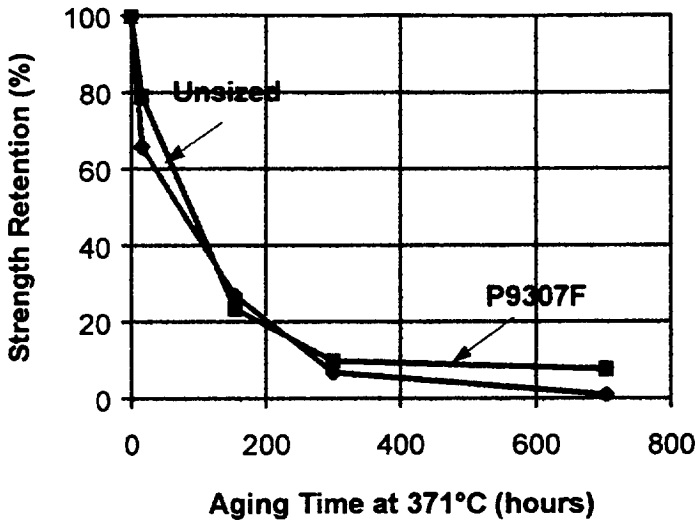

Figure 23. 90° flexural strength retention of T650-35/PMR-II-50 laminates

Weight losses of all the materials are too great for retention of significant mechanical properties, which shows that the aging conditions chosen are too severe for the PMR-II-50. Note that aging at 371°C (700°F) is more than 20°C above the composite Tgs given in Table VI. Environmental damage would be expected to be greater above T_g due to increased chain mobility and oxygen diffusion rates. The severe aging conditions are reflected in the post-exposure mechanical properties at room temperature given in Figures 22 and 23.

While the specimens corresponding to the data shown in Figures 22 and 23 are too severely degraded to have much meaning, they do show that the finishes, particularly the P9307F, provide improved TOS even under these severe conditions. Improved TOS is strikingly apparent upon observation of the transverse failure surfaces for the unsized and P9307F shown in Figures 24-27.

Figure 24. Transverse fracture surface of aged (700 hours, 371°C) unsized laminate

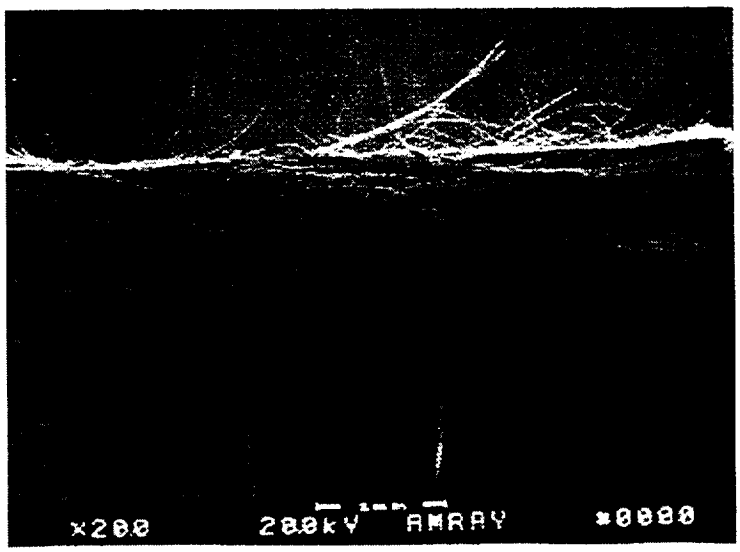

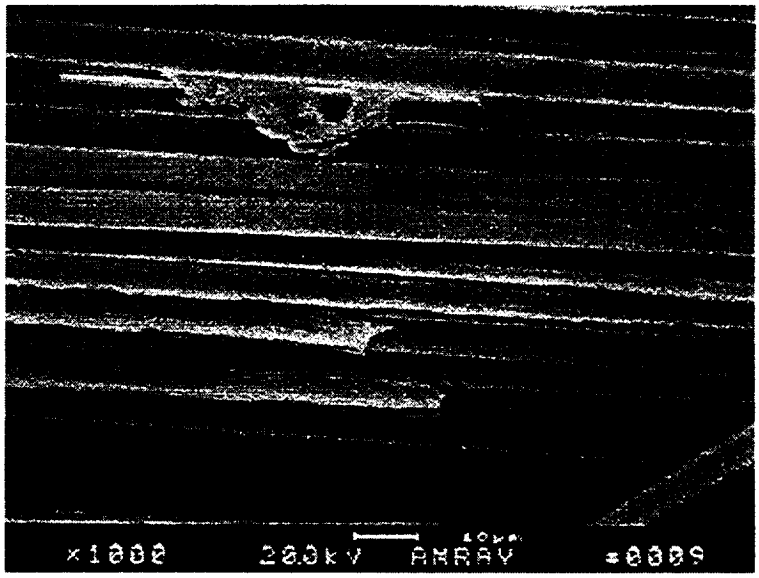

Figure 25. Magnified center section of Figure 24 showing interface-dominated failure

As seen in Figures 24-27, failure in the unsized material has become interface-dominated with numerous loose fibers in evidence on the fracture surface, while the finished material still shows matrix cohesive failure. Although the materials were severely degraded, these results show that the finishes have a positive effect on strength retention and protection of the interface.

Figure 26. Transverse fracture surface of aged (700 hours, 371°C) P9307F finished laminate

Additional insight into the reason for the precipitous drop in flexural strengths with aging time at 371°C (700°F) can be obtained by examination of the composite edges. Figures 28 and 29 show edge views of aged T650-35/PMR-II-50 composites as a function of aging time with unsized and P9307F finished fibers. Both types of composite show the formation of large surface cracks after 150 hours of aging. After

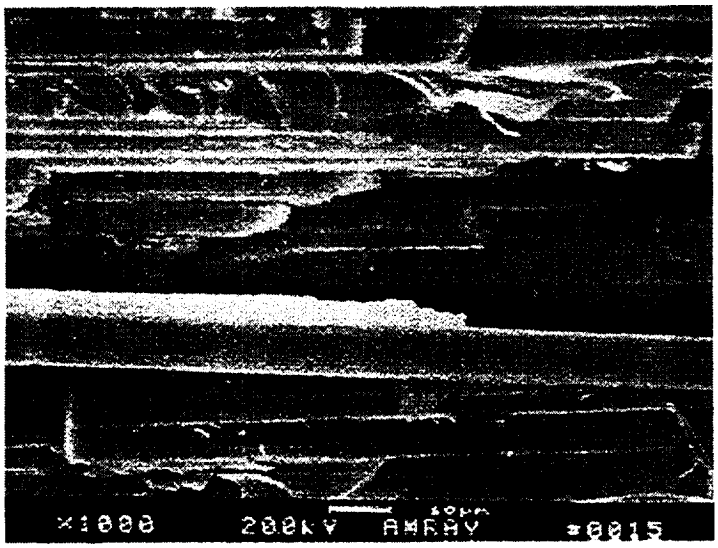

Figure 27. Magnified center section of Figure 26 showing matrix cohesive failure

300 hours, a deep darkened zone filled with large cracks and voids is visible. Seven hundred hours of aging results in virtual destruction of the surface with the unsized fibers (Figure 28) and a dark degraded zone on the P9307F finished material (Figure 29).

The lower strength loss and reduced surface cracking exhibited by the finished composites supports the original hypothesis that improving interfacial bonding will improve composite thermo-oxidative stability. It is expected that the beneficial effects of the finish will be more pronounced at lower exposure temperatures where the PMR-II-50 is more stable and the interfacial oxidation mechanism is more dominant.

To supplement the SEM observations, micro-FTIR spectra were taken on the 700-hour aged laminates and compared to the unexposed control samples for absorption band changes following exposure. The spectra taken from the finished specimens showed substantially more intensity for the resin-associated IR absorptions after aging than the spectra of the unsized material after exposure. All exposed sample spectra showed band shifts relative to the unexposed controls for those bands associated with the matrix resin. Two bands associated with the carbon fiber surface (1516.6 cm^{-1}, 1210 cm^{-1}) did not show these shifts with aging, although they did decrease in intensity after exposure. The spectral shift data are given in Table VIII together with the band assignment.

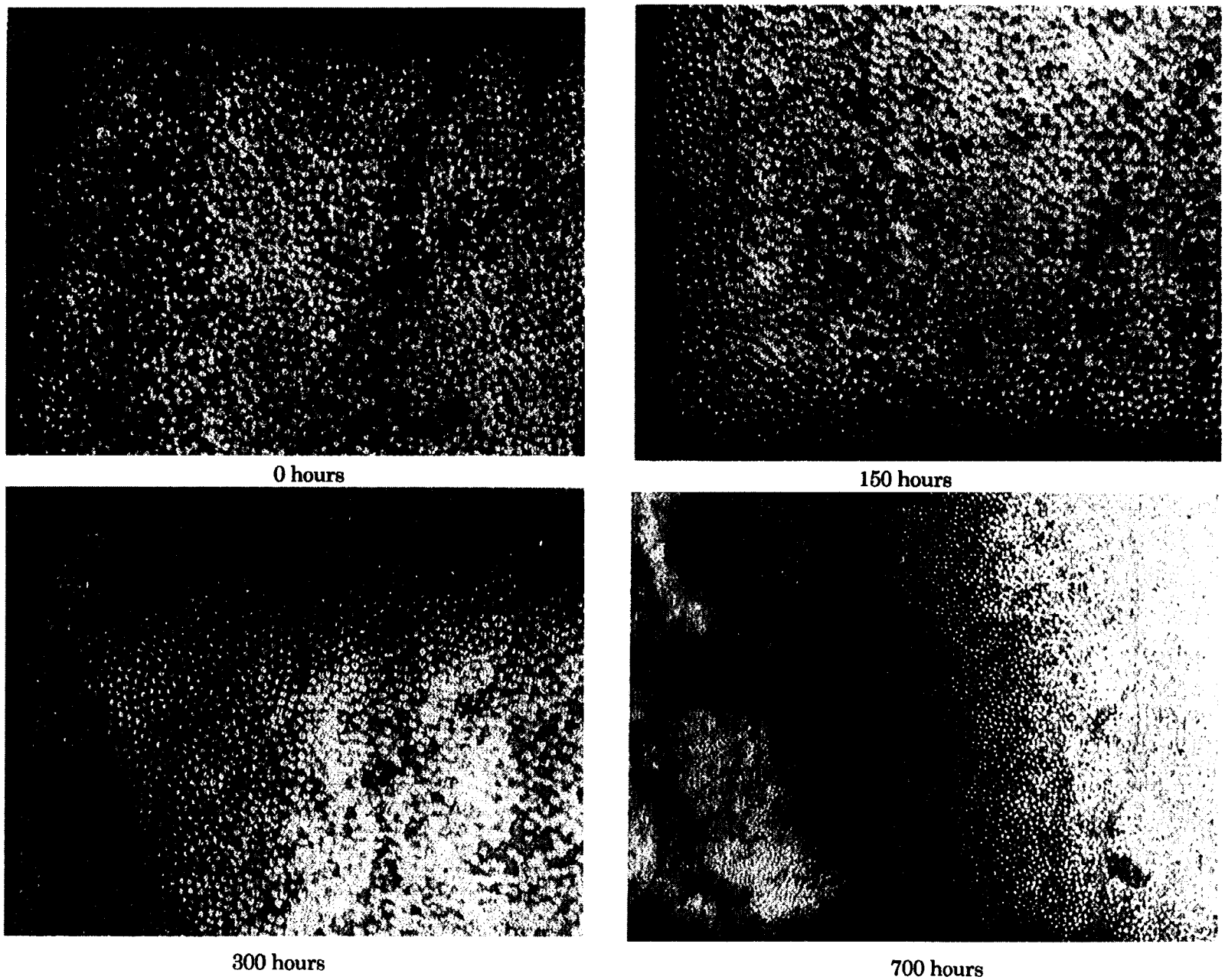

Figure 28. Edge view of T650-35/PMR-II-50 unsized laminate aged at 371°C

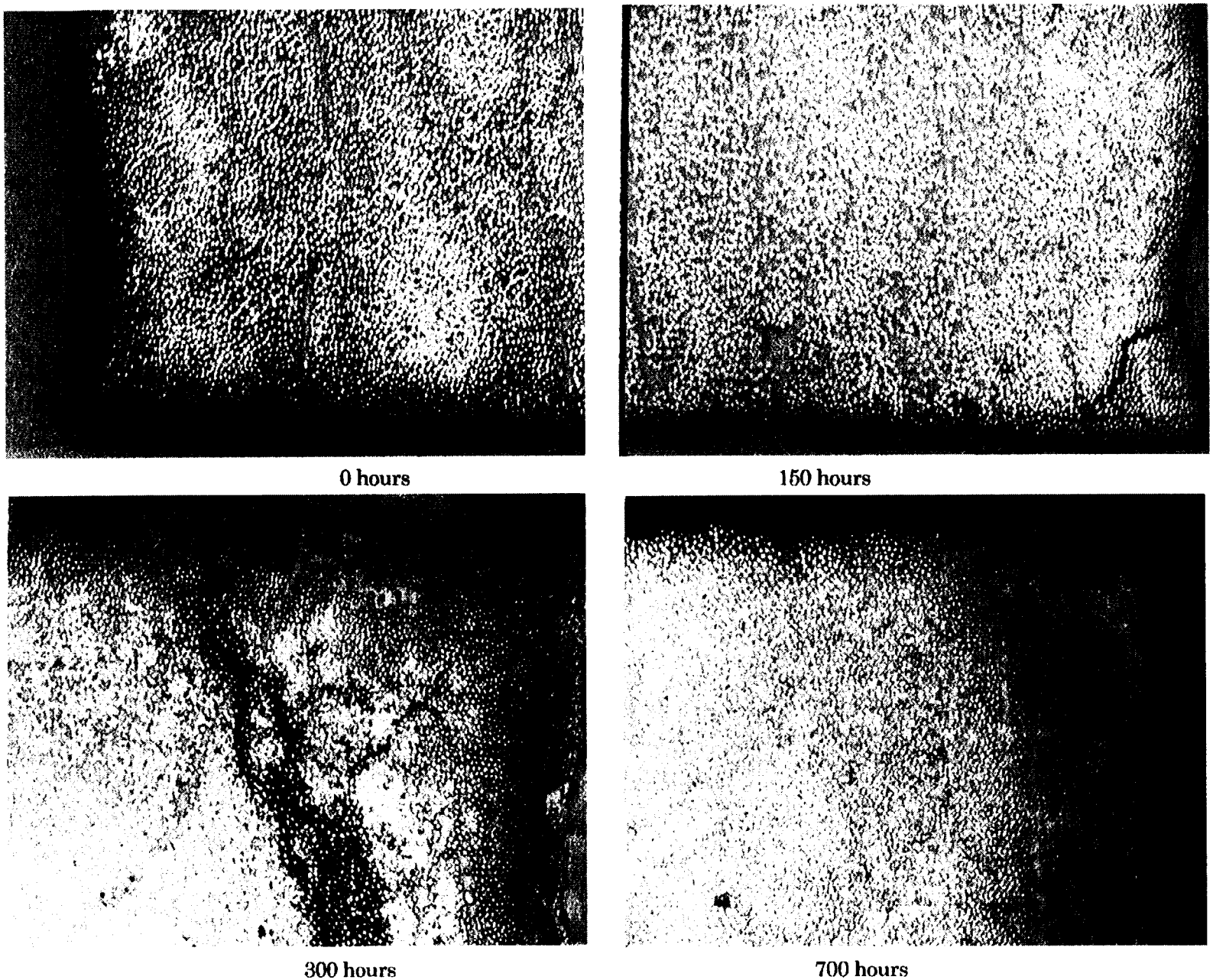

Figure 29. Edge view of T650-35/PMR-II-50 P9307 finished laminate aged at 371°C

Table VIII. Spectral Shifts Induced by Thermal Aging 700 Hours at 371°C

P9307F Finish			P9306F Finish			Unsized		
Unexp.	Exp.	Diff.	Unexp.	Exp.	Diff.	Unexp.	Exp.	Diff.
1723.1	1728.9	5.8	1726.9	1728.9	2.0	1726.9	1732.7	5.8
1516.6	1516.6	0	1516.6	1516.6	0	1516.6	n/o	--
1364.2	1362.2	-2.0	1364.2	1358.4	-5.8	1364.2	1362.2	-2.0
1258.1	1260.0	1.9	1258.1	1256.1	-2.0	1258.1	n/o	--
1211.7	1211.7	0	1211.7	1211.7	0	1209.8	1209.8	0
1196.3	1198.2	1.9	1190.5	1192.4	1.9	1194.4	n/o	--
723.6	727.4	3.8	721.6	723.6	2.0	725.5	n/o	--

Band assignment:

1720-1730	Imide carbonyl
1516.6	Surface ring deformation, fiber
1356-1364	V-F in resin
1256-1260	C-F, Imide ring stretch, resin, fiber surface oxidation
1209-1211	Surface bonded oxygen, fiber
1190-1198	Aromatic band in resin, shifts higher with aging probably as a result of increased ring substitution with oxidation
720-728	CF_3 deformation, aromatic C-H deformation

These IR data indicate that oxidation is occurring both in the resin bulk and at the fiber/matrix interface. The presence of finishes appears to limit degradation by inhibiting interface oxidation. The P9307F finish was more effective in oxidation inhibition than the P9306F. Spectra of P9307F finished material and the unsized material are shown in Figures 30 and 31, respectively.

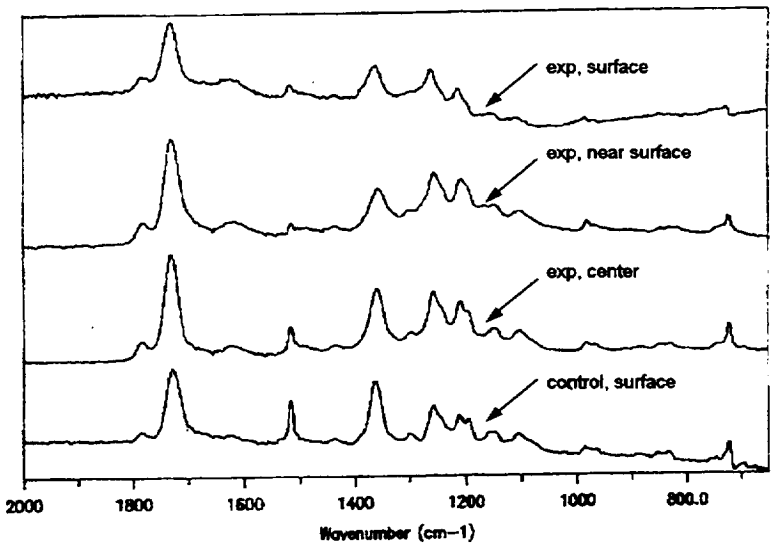

Figure 30. Infrared spectra of composite with P9307F finish aged 700 hours at 371°C

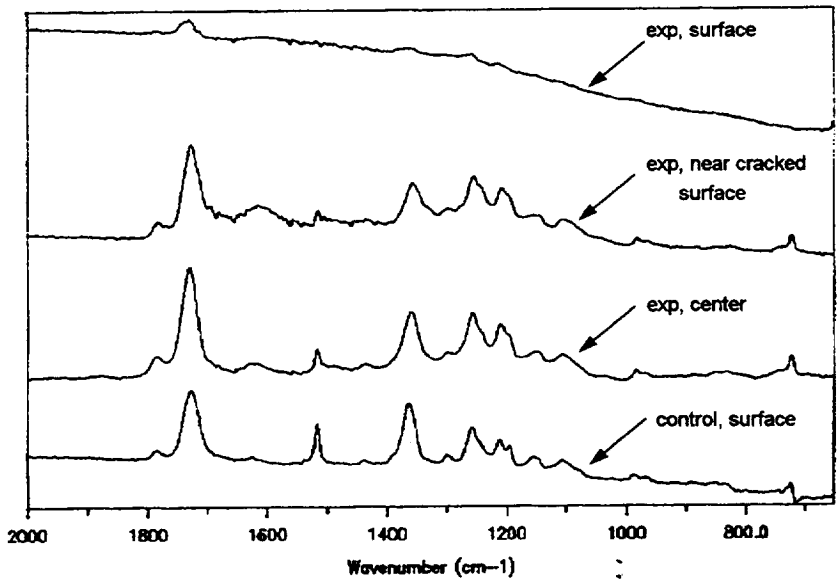

Figure 31. Infrared spectra of composite with unsized fibers aged 700 hours at 371°C

Although the specimens were overaged, the data still show that the finishes being studied in this program provide a significant amount of oxidation protection for the fiber/matrix interface. The mechanical property results are supported by results from VCXPS, DMA, optical and electron microscopy, and micro-FTIR. In every case, the P9307F finish provides performance superior to the unsized material. The IR data, in particular, show that the finish is inhibiting oxidation of both the fiber and matrix.

316°C Aging Study

In the last phase of the program, a limited number of specimens were exposed at 316°C (600°F). It was thought that this temperature was still an aggressive environment but was a more reasonable exposure condition based on earlier work. Additional prepregs were prepared and autoclave molded into unidirectional composite panels. Note that these panels were autoclave molded at 290 psi, which is at a lower pressure than that used in the press-molded laminates used in the 371°C (700°F) aging study. Panels that passed ultrasonic inspection were used in the aging studies. Longitudinal and transverse flexure specimens from composites containing unsized and P9307F finished fibers were aged at 316°C (600°F) following the same procedures as the previous aging studies.

After 1000 hours, the P9307F finished material showed a weight loss of 5.3% for the 0° specimens and 7.9% for the 90° specimens. The unsized 0° specimens had a weight loss of 3.1% and the 90° specimens showed a loss of 3.8%. The higher weight loss seen for the P9307F material is also reflected in the mechanical property results given in Table IX.

Table IX. Mechanical Properties of T650-35/PMR-II-50 Laminates Aged 1000 hours at 316°C

Surface Treatment	90°C Flexure MPa (ksi)	0° Flexure MPa (ksi)
Unsized Control	27.6 (4.0)	1060.5 ± 96.6 (153.7 ± 14.0)
P9307F Finish	20.7 ± 20.0 (3.0 ± 2.9)	807.3 ± 89.7 (117.0 ± 13.0)

No new as-produced material was tested from the materials used in the 316°C (600°F) aging tests. Compared to the as-fabricated mechanical properties given in Table VII, the unsized material showed a 73% strength retention in 0° flexure after 1000 hours aging at 316°C (600°F) and a 23% strength retention in 90° flexure. The P9307F material showed a 64% strength retention in 0° flexure and a 16% strength retention in 90° flexure. Thus, the finished material displayed similar aged strength retention despite having nearly twice as much weight loss.

In an effort to understand the 316°C (600°F) aging results, an extensive study of the composite microstructures was undertaken using optical microscopy, image analysis, and SEM. The microstructures of the specimens shown in Figure 32 indicated that the finished and unsized composites had similar initial void contents. Examination of photomicrographs of the 316°C (600°F) aged material also shown in

Figure 32 indicates increased void content and size in the unsized material but shows little change in microstructure in the P9307F finished material. End pieces from tested P9307F finished and unsized flexure specimens aged at 316°C (600°F) were then examined for porosity content by image analysis at 10-14 locations. Measured void contents and fiber volumes are given in Table X.

Table X. Image Analysis Results from 316°C Aging Specimens

Specimen Type	Void Content (%)	Fiber Volume (%)
Unsized, as-processed	1.21 ± 0.30	53.4
Unsized, aged 1000 hours	5.46 ± 2.59	43.2
Finished, as-processed	1.41 ± 0.60	55.6
Finished, aged 1000 hours	2.36 ± 0.88	53.6

The image analysis results given in Table X show no apparent reason for the higher weight loss displayed by the P9307F finished material. A low fiber volume or a high void content could produce the observed weight loss behavior, but those properties are close to those of the unsized material. Care should be taken in interpretation of these results. Although qualitatively the observations of higher void content in the unsized samples compared to the finished samples describe the microstructure, the sampling procedures used in the image analysis may skew estimates of void content. The low measured fiber volume for the aged unsized material demonstrates that sampling procedures need to be expanded to more locations.

SEM analyses on the same polished samples indicated that the finished material had a higher microcrack density than the unsized materials in the control as well as in the exposed condition (Figures 33 and 34). The difference in microcrack density may be due to the improved adhesion in the finished sample, which precludes the relief of residual stress in the composite by interfacial debonding. In addition, the higher void content in the unsized materials may similarly have acted to relieve internal stress. Inspection of microcrack density in all of the samples indicated that local density was very low in regions of porosity in the laminate. The consequence of the higher microcrack density could be a faster general degradation and weight loss. A modification of the composite cure cycle may be required to reduce microcracking in the finished materials.

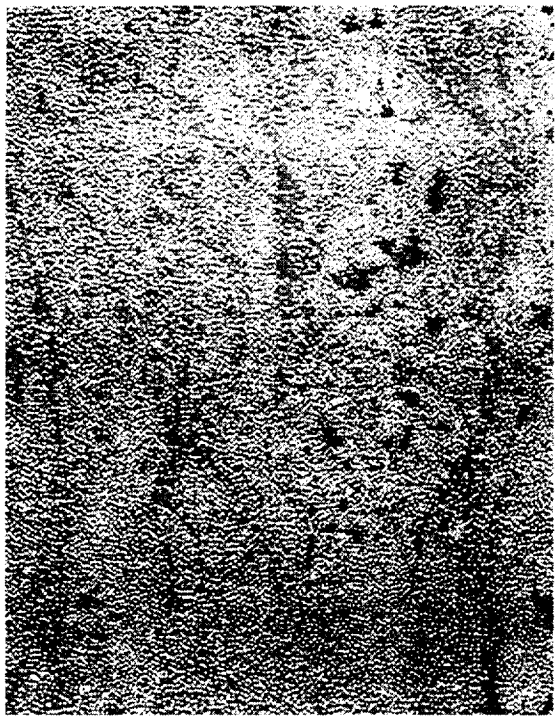

(a) unsized, as processed

(b) P9307F finish as processed

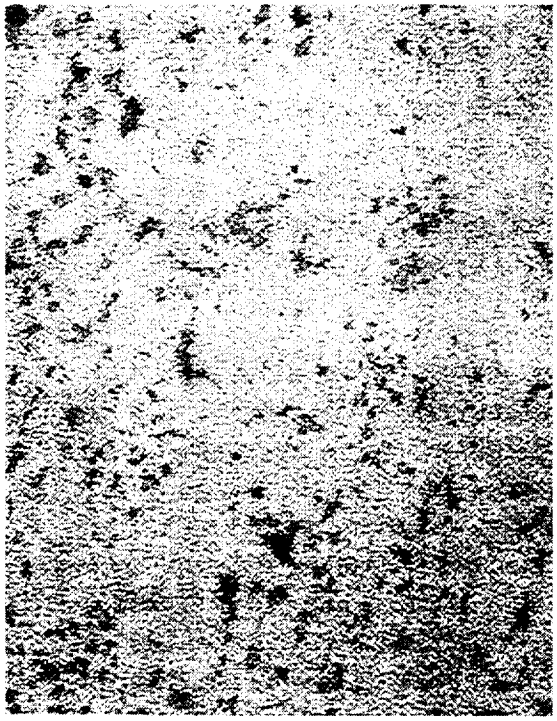

(a) unsized, 1000 hours, 316°C

(b) P9307F finish, 1000 hours, 316°C

Figure 32. Cross-sections of unsized and P9307F finished composites as processed and after 1000 hours at 316°C

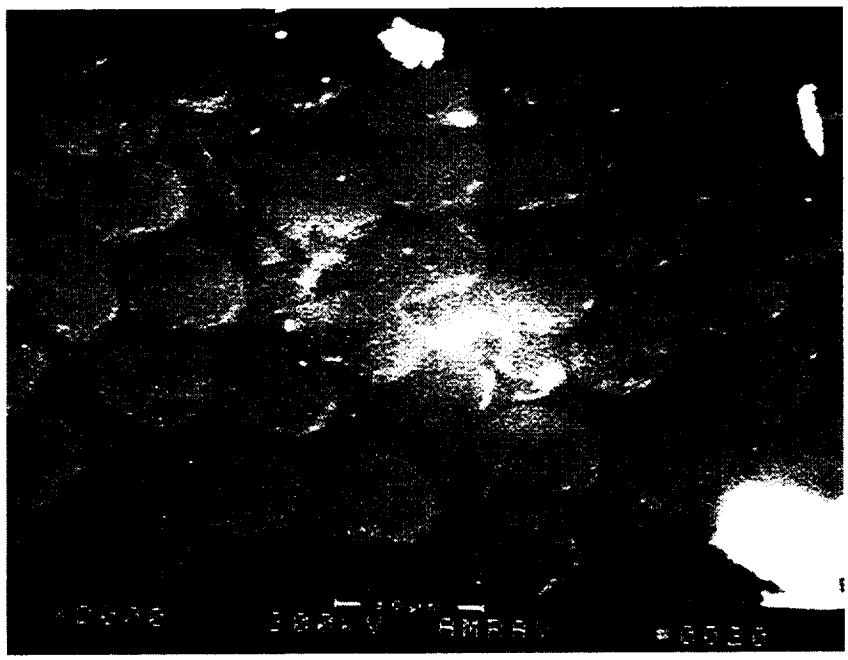

(a) unsized

(b) P9307F finish

Figure 33. SEM micrographs of T650-35/PMR-II-50 composites aged 1000 hours at 316°C

For comparison purposes, the specimens prepared by hot press molding at 500 psi for the 371°C (700°F) aging study were also examined for microcrack density using SEM. A very low microcrack density was observed in both the unsized and P9307F finished materials. Where microcracks were observed, they were located near the center of the laminates. There appeared to be more microcracks in the P9307F finished material although only a few microcracks were present. Representative microstructures of the hot press molded laminates are shown in Figure 34.

It appears that the lower microcrack density in the hot press molded laminates reduces the area of the matrix exposed to the oxidizing environment and reduces the rate of bulk weight loss. Without the presence of the microcracks, the interface becomes a larger contributor to composite TOS. In that case, the benefit of the P9307F finish is seen in a lower rate of weight loss as shown in Figure 21.

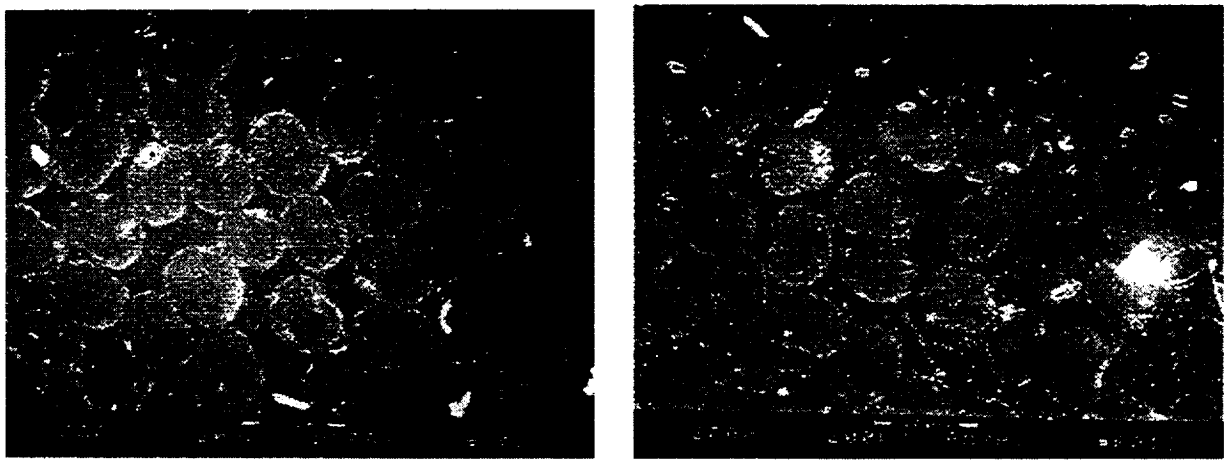

(a) unsized (b) P9307F finish

Figure 34. SEM micrographs of hot press molded T650-35/PMR-II-50 composites

Summary and Conclusions

Results from this program to demonstrate the use of reactive finishes for improving composite TOS are encouraging but not conclusive. The finishes were successfully formulated for uniformly coating the individual carbon fibers in a 3K tow and reacting with the T650-35 fiber and the PMR-II-50 polyimide matrix. Those formulations also displayed thermal stabilities near those of the neat PMR-II-50 material. Composites fabricated using finished fibers displayed mechanical properties similar to those fabricated using unsized fibers. When those composites were aged at 400 and 371°C (700°F), however, only limited evidence was obtained showing that the reactive finishes protect the fibers from oxidation and improve composite TOS. Those aging temperatures are above the matrix Tg, which leads to bulk degradation, and are too severe to obtain meaningful mechanical property results

on aged composites. Indirect evidence gathered on the aged composite fracture surfaces using SEM, micro-FTIR, DMA, and VCXPS techniques show that the finish reduces interfacial oxidation and support the hypothesis that the finish improves composite TOS.

Composite specimens aged at 316°C (600°F) displayed the opposite behavior from those aged at higher temperatures. Those samples were also observed to have a higher microcrack density in the finished material as fabricated. Processing differences between the composites aged at 371°C (hot press molded at 500 psi) and 360°C (autoclave molded at 290 psi) may be the cause of the higher microcrack density. The microcracks may be due to improved adhesion in the finished material that prevents relief of residual stresses by interfacial debonding. If so, modified cure cycles would have to be developed for the composite containing the reactive finishes. Additional work is required to explain this anomaly.

We must conclude that the evidence supporting the potential benefits of the reactive finishes is compelling, but not proven at this point. Results show that small changes in composite quality can dramatically change TOS. That shows the necessity for thoroughly characterizing the material before thermal aging. The results also show the desirability of using large numbers of samples and statistical analysis in these types of aging studies in order to obtain meaningful data. If these reactive finishes are proven to improve composite TOS, then their use will result in composites for high-temperature applications with greater environmental durability that should result in longer operating lifetimes.

Acknowledgments

The authors would like to thank Dr. James K Sutter at NASA LeRC for his guidance and insights throughout the program and for coordinating the work done at NASA LeRC in support of the project. We would also like to thank Mr. Doug Jaynes at NASA LeRC for conducting the VCXPS measurements and developing the battery biasing technique that made the measurements meaningful on fluorinated polymers.

References

1. T. T. Serafini, P. Delvigs, and G. R. Lightsey, "Thermally Stable Polyimides from Solutions of Monomer Reactants," *J. Appl. Polymer Sci., 16,* 4, 1972, pp. 905-906.

2. R. D. Vannucci, "PMR Polyimide Compositions for Improved Performance at 371°C," *SAMPE Quarterly, 19,* 1, October 1987, pp. 31-36.

3. K. J. Bowles, "A Comparison of Fiber Effects on Polymer Matrix Composite Oxidation," NASA TM 104416, NASA Lewis Research Center, Cleveland, OH, 1991.

4. D. A. Scola, J. H. Vontell, and B. L. Laube, "Relationship Between Graphite Fiber Surface Chemistry, PMR-15 Composite Shear Strength, and Thermooxidative Stability," *Proc. 33rd International SAMPE Symposium*, Society for the Advancement of Material and Process Engineering, Covina, CA, 1988, pp. 1506-1518.

5. J. D. Miller, R. A. Gray, D. Ward, J. B. Barr and W. C. Harris, "Relating Thermo-Mechanical Performance to Carbon Fiber/Matrix Adhesion in PMR-15 Laminates," *Proc. High Temple Workshop XIII*, 1993.

6. K. J. Bowles, M. Madhukar, and D. S. Papadopoulos, "Thermo-Oxidative Stability of Graphite/PMR-15 Composites: The Effects of Fiber Surface Modification on Composite Mode II Fracture Toughness," *Proc. 40th International SAMPE Symposium*, Society for the Advancement of Material and Process Engineering, Covina, CA, 1995, pp. 1879-1892.

7. R. Kuhbander, "Proceedings of High Temple Interface Task Force," Wright Laboratory Report WL-TR-93-4112, November 1993.

8. D. W. McKee and V. J. Mimeault, *Chemistry and Physics of Carbon*, Vol. 8, P. L. Walker and P. A. Thrower, eds., Marcel Dekker, NY, 1973, p. 151.

9. G. E. Hammer and L. T. Drzal, *Appl. Surface Sci., 4*, 1980, p. 340.

10. L. T. Drzal, M. J. Rich, and W. Ragland, *42nd Annual Conference Composites Institute*, Society of the Plastics Industry, 1987, pp. 1-4.

11. R. E. Allred and L. A. Harrah, *Proc. 34th International SAMPE Symposium*, Society for the Advancement of Material and Process Engineering, Covina, CA, 1989, p. 2559.

12. A. E. Bolvari and T. C. Ward, *Inverse Gas Chromatography: Characterization of Polymers and Other Materials*, D. R. Lloyd, T. C. Ward and P. Schreiber, eds., American Chemical Society, ACS Series 391, 1989, pp. 217-229.

13. J. D. H. Hughes, *Composite Sci. Tech., 41*, 1991, pp. 13-45.

14. R. E. Allred and W. C. Schimpf, "CO_2 Plasma Modification of High Modulus Carbon Fibers and Their Adhesion to Epoxy Resins," *J. Adhesion Sci. Tech.*, 8, 4, 1994, pp. 383-394.

15. A. Ishitani, *Carbon, 19*, 4, 1981, pp. 269-275.

16. E. Fitzer and R. Weiss, *Carbon, 25*, 4, 1987, pp. 455-467.

17. S. Wang and A. Garton, *Proc. American Chemical Society, Division of Polymeric Materials: Science and Engineering, 62*, 1990, pp. 900-902.

18. L. T. Drzal, M. J. Rich, M. F. Koenig, and P. F. Floyd, *J. Adhesion, 16*, 1983, pp. 133-152.

19. J. G. Williams, M. E. Donnellan, M. E. Janes, and W. L. Morris, *Interfaces in Composites*, C. G. Patano and E. J. Chen, eds., Materials Research Society, Pittsburg, PA, *170*, 1989, pp. 285-290.

20. F. J. McGarry and J. E. Moalli, *SAMPE Quarterly, 23*, 4, 1992, pp. 35-38.

21. S. H. Jao and F. J. McGarry, *J. Reinforced Plastics and Composites, 11*, 1992, pp. 811-832.

22. J. Chang, J. P. Bell and R. Joseph, *SAMPE Quarterly, 18*, 3, 1987, pp. 39-45.

23. M. Labronici and H. Ishida, *Proc. 4th Intl. Conf. Composite Interfaces*, 1992, p. 33.

24. K. C. Chuang and J. E. Waters, "Effects of Endcaps on the Properties of Polyimide/Carbon Fiber Composites," *Proc. 40th Intl. SAMPE Symposium*, Society for the Advancement of Material and Process Engineering, Covina, CA, 1995, pp. 1113-1123.

REPORT DOCUMENTATION PAGE

Form Approved
OMB No. 0704-0188

1. AGENCY USE ONLY (*Leave blank*)	2. REPORT DATE	3. REPORT TYPE AND DATES COVERED
	July 1997	Final Contractor Report

4. TITLE AND SUBTITLE

Fiber Finishes for Improving Interfacial Thermo-Oxidative Stability in PMR-II-50 Matrix Composites

5. FUNDING NUMBERS

WU-523-21-13
C-NAS3-27090

6. AUTHOR(S)

Ronald E. Allred, Larry A. Harrah, Thomas A. Donnellan, Theotis Williams, Jr., and Raymond Meilunas

7. PERFORMING ORGANIZATION NAME(S) AND ADDRESS(ES)

Adherent Technologies, Inc.
9621 Camino del Sol NE
Albuquerque, New Mexico 87111
and
Northrop Grumman Corporation
Advanced Technology Development Center
Bethpage, New York 17114

8. PERFORMING ORGANIZATION REPORT NUMBER

E-10733

9. SPONSORING/MONITORING AGENCY NAME(S) AND ADDRESS(ES)

National Aeronautics and Space Administration
Lewis Research Center
Cleveland, Ohio 44135-3191

10. SPONSORING/MONITORING AGENCY REPORT NUMBER

NASA CR-202343

11. SUPPLEMENTARY NOTES

Project Manager, James K. Sutter, Materials Division, NASA Lewis Research Center, organization code, 5150, (216) 433-3226.

12a. DISTRIBUTION/AVAILABILITY STATEMENT

Unclassified - Unlimited
Subject Category 24

This publication is available from the NASA Center for AeroSpace Information, (301) 621-0390.

12b. DISTRIBUTION CODE

13. ABSTRACT ***(Maximum 200 words)***

The interface has been shown to be a preferential site for thermo-oxidative degradation in carbon/polyimide composites. This study entails the development and demonstration of improved T650-35 carbon/PMR-II-50 polyimide composites through the use of high-temperature finishes. The finishes are based on a family of novel difunctional coupling agents that have been shown to form chemical bonds with a variety of organic, inorganic, and metallic materials. The finishes consist of a mixture of these coupling agents, PMR-II-50 carrier, surfactant, and solvent. A solvent dip process is used to apply the finishes. Subsequent application of heat dries the solvent and initiates reaction between the finish and the fiber. As applied, the finishes form a uniform 0.5μ coating on each fiber that cannot be removed by a methanol wash and remain flexible for subsequent processing. When incorporated into a polyimide matrix composite, the finish reacts with the matrix resin during processing to form chemical bonds in the interphase. This approach has the potential to dramatically improve thermo-oxidative stability (TOS) of the interface in polyimide-matrix composites. The addition of these finishes to fiber surfaces serves the dual purpose of protection of the fiber during handling and alteration of the interphase in the cured composite. Initial results show that the finishes are compatible with PMR-II50 processing and bond well to carbon fibers. The finishes display excellent TOS. Aged composites with these finishes show good retention of mechanical properties. Microinfrared spectroscopy indicates that oxidation of the carbon fiber surfaces is reduced in composites containing finished fibers.

14. SUBJECT TERMS

Polymides; Finishes; Sizings; Graphite fiber composites

15. NUMBER OF PAGES

53

16. PRICE CODE

A04

17. SECURITY CLASSIFICATION OF REPORT	18. SECURITY CLASSIFICATION OF THIS PAGE	19. SECURITY CLASSIFICATION OF ABSTRACT	20. LIMITATION OF ABSTRACT
Unclassified	Unclassified	Unclassified	